How to cite: *Angew. Chem. Int. Ed.* **2023**, *62*, e202301909
doi.org/10.1002/anie.202301909

Biomass Valorization

Radical-Mediated Photocatalysis for Lignocellulosic Biomass Conversion into Value-Added Chemicals and Hydrogen: Facts, Opportunities and Challenges

*Dominic Aboagye, Ridha Djellabi, Francesc Medina, and Sandra Contreras**

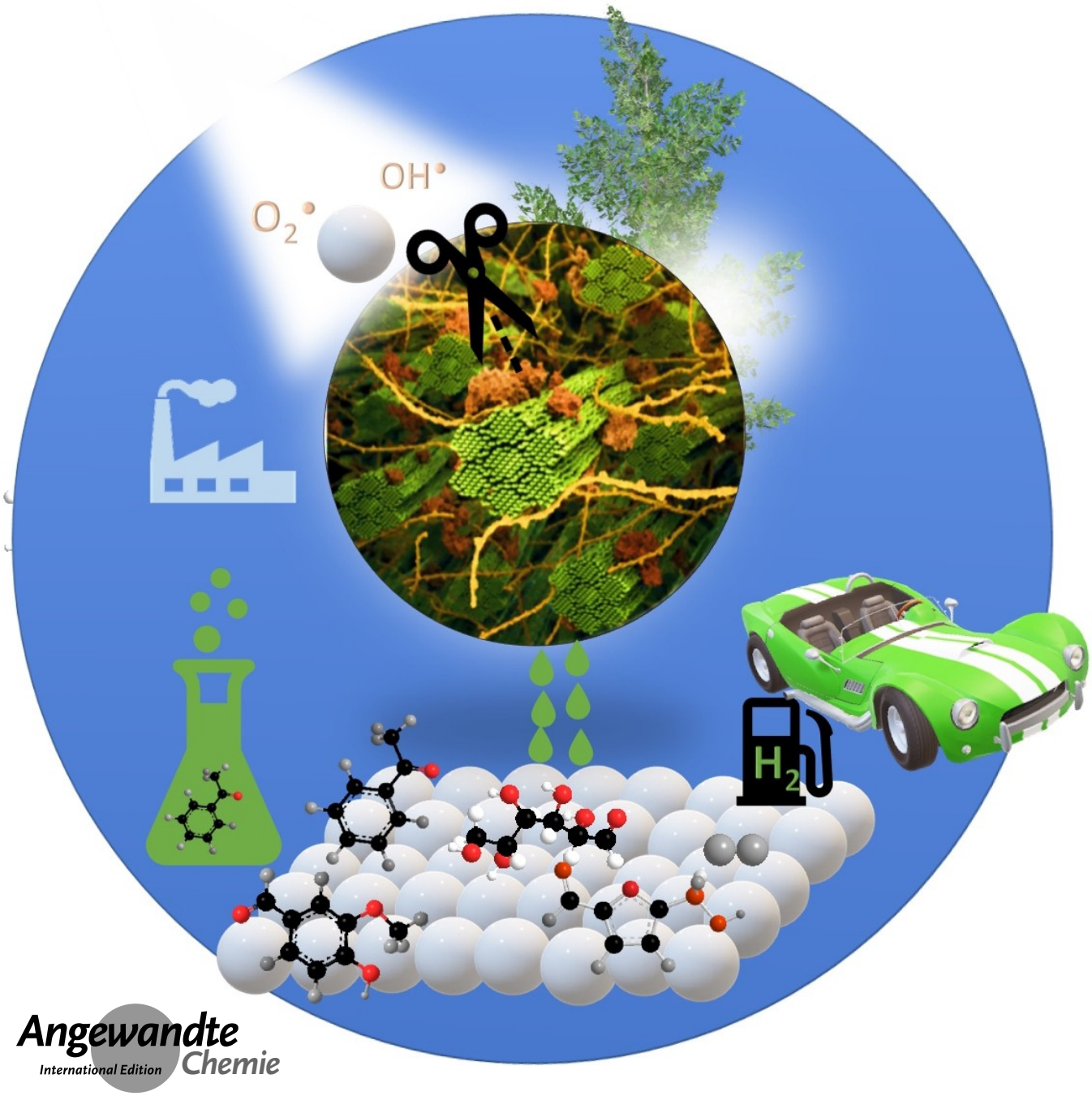

Abstract: Photocatalytic biomass conversion into high-value chemicals and fuels is considered one of the hottest ongoing research and industrial topics toward sustainable development. In short, this process can cleave C_β–O/C_α–C_β bonds in lignin to aromatic platform chemicals, and further conversion of the polysaccharides to other platform chemicals and H_2. From the chemistry point of view, the optimization of the unique cooperative interplay of radical oxidation species (which are activated via molecular oxygen species, ROSs) and substrate-derived radical intermediates by appropriate control of their type and/or yield is key to the selective production of desired products. Technically, several challenges have been raised that face successful real-world applications. This review aims to discuss the recently reported mechanistic pathways toward selective biomass conversion through the optimization of ROSs behavior and materials/system design. On top of that, through a SWOT analysis, we critically discussed this technology from both chemistry and technological viewpoints to help the scientists and engineers bridge the gap between lab-scale and large-scale production.

1. Introduction

The growing global concerns over rapid resource depletion, climate change, and species extinctions have driven a paradigm shift from a linear-based economy to utilizing a circular bioeconomy approach. The circular bioeconomy portfolio is expected to unlock the full potential of resources sustainably.[1,2] Biomass resource is estimated to be 181.5 billion tonnes annually, making it the largest renewable energy resource globally.[3] However, out of this, only 3 % has been successfully incorporated into the ongoing circular bioeconomy concept.[3] Biomass offers enormous potential for sustainable chemicals to replace petroleum-based sources. Conversion of biomass to desired chemicals generally requires efficient protocols and strategies, which can selectively cleavage of the bonds within the biomass substrate or enable the controlled upgrade of biomass-derived platforms.

In lignocellulose biorefinery, techniques such as alkaline or acid pretreatment, ozonolysis, partial or hot water wet oxidation, oxidative/reductive, organosolv, among others are used for separating lignin (called native lignin) and polysaccharides.[4,5] Biomass conversion leads to several product streams and this may vary depending on the fraction of biomass (cellulose, hemicellulose, and lignin). For instance, lignin is considered the largest single source of aromatic building blocks, thereby making its valorization one of the most highly researched areas.[6,7] Selective oxidation of C–O and C–C bonds in lignin could release valuable platform chemicals such as benzene, toluene, xylene (BTX) and phenolic monomers such as catechol, guaiacol, vanillin, syringaldehyde, p-hydroxybenzaldehyde, syringic acid, ferulic acid, vanillic acid, among others.[8] Moreover, the oxidation of polysaccharides to different downstream products such as 5-hydroxymethylfurfural (HMF) can also produce 2,5-Furandicarboxylic acid (FDCA). HMF itself is a key platform chemical that can be upgraded to produce chemicals and fuels.[9]

The conversion of lignocellulosic biomass (LCB) to value-added chemicals and fuels has been achieved through biochemical, thermochemical, or microbial strategies, and each has its pros and cons. Thermocatalytic conversion of LCB has been well established as a key LCB conversion process.[10,11] However, the high reaction temperature and high pressure employed lead to the formation of unfunctionalized aromatics, alcohols, or alkanes.[12] Pyrolysis/gasification of LCB typically results in the production of syngas (CO and H_2), and extensive bond cleavage, which results in the removal of key functional groups in monomers, yielding simplified aromatics and low-value chemicals.[13] Extensively de-functionalized products may require further re-functionalization for high-value chemicals, rendering the process atom inefficient and energy-consuming. As a hotspot in biomass research, recent efforts are targeted at the development of milder conversion strategies that can fully convert biomass fractions (lignin and polysaccharides) to chemicals and fuels. Hydrogen has been targeted as a promising clean and potentially renewable alternative to fossil fuels.[14–16]

Therefore, photocatalysis as an eco-friendly technique is targeted as an emerging LCB conversion route.[17–19] The so-called term "soft/mild radical oxidation" is usually used to describe photocatalytic biomass conversion.[20,21] Photogenerated (electrons and holes) could activate molecular oxygen to radical oxygen species (ROSs) ($^\bullet O_2^-$, H_2O_2, $^\bullet OH$, alpha-oxygen and singlet oxygen). These ROSs are reactive and short-lived, and they usually attack specific atoms in organic substrates generating substrate-based radical intermediates such as alkoxy radical ($RO^\bullet$), hydroperoxide (RO_2H), peroxy radical ($RO_2^\bullet$), among others.[22,23] The substrate-based radical intermediates could also undergo further reaction with activated molecular oxygen species to form desired products. In biomass conversion systems by photocatalysis, a tradeoff between the yield and the nature of photoproduced ROSs is required to produce selectively the desired products with less side reactions, i.e., over-oxidation of products.[24] Based on the nature of biomass substrate, one of multi-steps radical oxidation can take place to reach the targeted product. Within these steps, both the nature and the yield of ROSs is crucial and improper generation of

[*] D. Aboagye, Dr. R. Djellabi, Prof. F. Medina, Dr. S. Contreras
Departament d'Enginyeria Química, Universitat Rovira i Virgili
Av. Països Catalans 26, 43007 Tarragona (Spain)
E-mail: sandra.contreras@urv.cat
Homepage: https://twitter.com/cienciaURV

ROSs would affect the selectivity or disturb the overall process. One has it the control of ROSs behavior could be obtained through the optimization of reaction parameters such as the quantity of photocatalyst, time of reaction, addition of ROSs scavengers and so on. The other concept aims to design heterojunction semiconductor systems with different redox abilities to generate smartly the required amount and yield of targeted ROSs. While high performing photocatalysts have been designed to promote evolution of solar H_2 via water splitting (without biomass), the need for sacrificial reagents(hole scavengers), along with sluggish reaction kinetics and low quantum yields of H_2 ($\approx$1.8 %) have impeded effective expansion of this technology.[25] As an alternative to conventional sacrificial reagents, biomass can be used as a low-cost alternative material to scavenge photogenerated holes to produce H_2 and concomitantly produces value-added chemical.[26] Recently, the properties of catalyst and reaction conditions are tuned for controlling radicals which is also gaining key interest.[27] Over the past decade, the merging of transition metals with photoredox photocatalysts via a process called metallaphotocatalyst has been one key route for controlling the generation and interaction of radical intermediates in most protocols designed for photocatalytic organic transformation reactions.[28,29] In this sense, the synthesis routes, type of selected semiconductors and ratios are very important parameters. ROSs can be managed as well via the modification of the photocatalyst surface. Another approach to control the behavior of generated ROSs is the involvement of new catalytic processes to the photocatalytic systems, such as design of photocatalytic materials which can produce heat which in turn has a direct effect on the role of generated ROSs.

Several previous reviews have been reported to discuss the photocatalytic conversion of biomass into valuable products.[20,21,30] Currently, the major efforts of the scientific community are devoted to finding the appropriate response to the raised question "How to control such a tradeoff?" Several contemporary studies have addressed this fact from different visions. Recently, Huang et al.[30] have reviewed interesting strategies for controlling substrate-based radical intermediates with significant attention paid to lignin bond cleavage from the chemistry point of view. The review is very inspiring and it would help researchers to understand the systematic role of radical intermediates in biomass conversion to value-added chemicals. Controlling the interplay between ROSs from molecular oxygen activation and substrate-based radical intermediates and an expanded summary of the industrial feasibility of this technology for biomass conversion is needed. The present review discusses the recent news on the strategies and experimental mechanisms via the unique cooperative interplay of ROSs from molecular oxygen activation and substrate-derived radical intermediates, for promoting biomass selective bond activa-

Dominic Aboagye is currently a Marti Franquès Predoctoral Fellow at the Department of Chemical Engineering, Universitat Rovira i Virgili, Tarragona (Spain). Dominic received his M.Sc. (2016) from Makerere University in Uganda. His ongoing Ph.D. is under the supervision of Dr. Sandra Contreras and Prof. Francesc Medina. His research interests are heterogeneous catalysis, biomass valorization, and technologies for wastewater treatment. His current research is on the development of photocatalytic approaches for the oxidation of lignin to value-added platform chemicals.

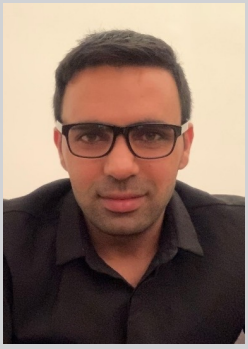

Ridha Djellabi received his PhD from Badji-Mokhtar University (Algeria) in Analytical Chemistry and Environment in collaboration with ISMER Lab (University of Milan, Italy). He then carried out his postdoctoral research at LSRE-University of Porto, Portugal. After that, Ridha joined REDOX group-Research centre for eco- environmental sciences, Chinese Academy of Sciences (Beijing, China) and Shenzhen University (Shenzhen, China). Then, Ridha joined ISMER group University of Milan (Italy) as a researcher. Currently, Ridha is a Maria Zambrano research fellow at Department of Chemical Engineering, Universitat Rovira i Virgili, Tarragona, Spain. Ridha does research about solar materials design for photocatalytic and photothermal applications.

Francesc Medina obtained his Ph.D. in 1993 from Rovira i Virgili University (URV). He joined URV as a lecturer in 1997 and he was awarded by ICREA Academia with a "Distinguished Professor Award" in 2009. He directs the Heterogeneous Catalysis research group (CATHETER) of URV since 2007, the director of R+D of the TECNIO innovation centre AMIC since 2003 and the co-founder and director of the spin-off company APLICAT S.L. He has participated in 129 competitive projects of the Spanish, Catalan and European governments, and more than 200 projects of technology transfer with companies.

Sandra Contreras obtained her PhD in Chemical Engineering from Universitat de Barcelona (UB) in 2003. From 2003 to 2005 she was in charge of the management and promotion of the CEQAP Innovation Centre from the Department of Chemical Engineering, UB. In 2005 she joined the ASCAMM Foundation Technology Center as European Project Manager. She joined the Dept. of Chemical Engineering at Universitat Rovira i Virgili in 2007 as Ramon y Cajal Researcher Fellow, becoming an Associate Professor-Serra-Húnter Fellow in 2015. Her research interests include water and wastewater treatment and reuse, advanced oxidation processes, heterogeneous catalysis and photocatalysis, and biomass valorisation.

tion and fragmentation to value-added chemicals and the concomitant evolution of hydrogen and value-added chemicals from both academic and industrial viewpoints. Under these discussions, the review focuses on the photocatalytic conversion of biomass (including cellulose, lignin, hemicellulose), hydrolysis of polysaccharides to monosaccharides (including glucose, xylose, etc.) via plasmonic photocatalysis strategy, and partial oxidation of biomass derivatives (furanic compounds such as HMF) and hydrogen evolution routes as summarized (Figure 1). In addition, a SWOT analysis was provided to clarify the main cons and pros of this technology for larger transfer to real-world application.

2. Photocatalysis Application and Fundamental Role of Radical Oxygen Species

2.1. Role of radical oxidation species in photocatalytic reactions

The heterogeneous photocatalytic process can provide redox power to the medium, instead of stoichiometric oxidant/reductant homogeneous reagents, through activation of molecular oxygen, the formation of several reactive oxygen species (ROSs) mostly on the surface of the photocatalyst occurs. Photocatalytic reactions begin with the photoexcitation of a photocatalyst by light irradiation, having an energy equal to or greater than the band gap of the semiconductor photocatalyst, which allows the formation of positive holes and electrons on the valence and conduction bands, respectively. However, not only is photoexcitation important in photocatalytic systems but also the rate of e^-/h^+ separation and VB and CB versus the potential of O_2 and H_2O to produce ROSs. Photocatalytic redox towards the oxidation or reduction of species in a medium are dependent on thermodynamic factors.[31] For the oxidation of a chemical substrate, the energetic level of the valence band of the photocatalyst must be more positive than the substrate, while for the reduction, the conduction band's energetic level must be more negative as compared to the potential of the substrate to be reduced. In terms of ROSs generation by photocatalytic means, in general, the type and the yield of produced ROSs depend on the type of used photocatalyst under given conditions. In terms of ROSs generation by photocatalytic means, in general, the type and the yield of produced ROSs depend on the type of used photocatalyst under given conditions. Overall, the main photocatalytically produced ROSs including superoxide ($^{\bullet}O^-_2$, redox potential: +0.89 V, half-life 10^{-6} s), peroxides (H_2O_2, redox potential 1.78 V, very stable), hydroxyl radical ($^{\bullet}OH$, redox potential +2.81 V vs. standard hydrogen electrode, SHE, half-life 10^{-10} s), alpha-oxygen and singlet oxygen. The conversion of LCB to high-value products by photogenerated ROSs is very complicated and challenging. In fact, up to date, there is no conclusive evidence regarding the type of ROS for selective oxidation of LCB and more experimental research is recommended to optimize the oxidative conditions to boost the generation of a high yield of value-added chemicals. Some reports have concluded that mild oxidative $^{\bullet-}O_2$ would be more selective for the photoconversion of LCB as compared to highly oxidative $^{\bullet}OH$.[32] On top of that, it is important to point out that the origin and the fraction are also important keys to be taken into consideration as they can affect the mechanism of photo-

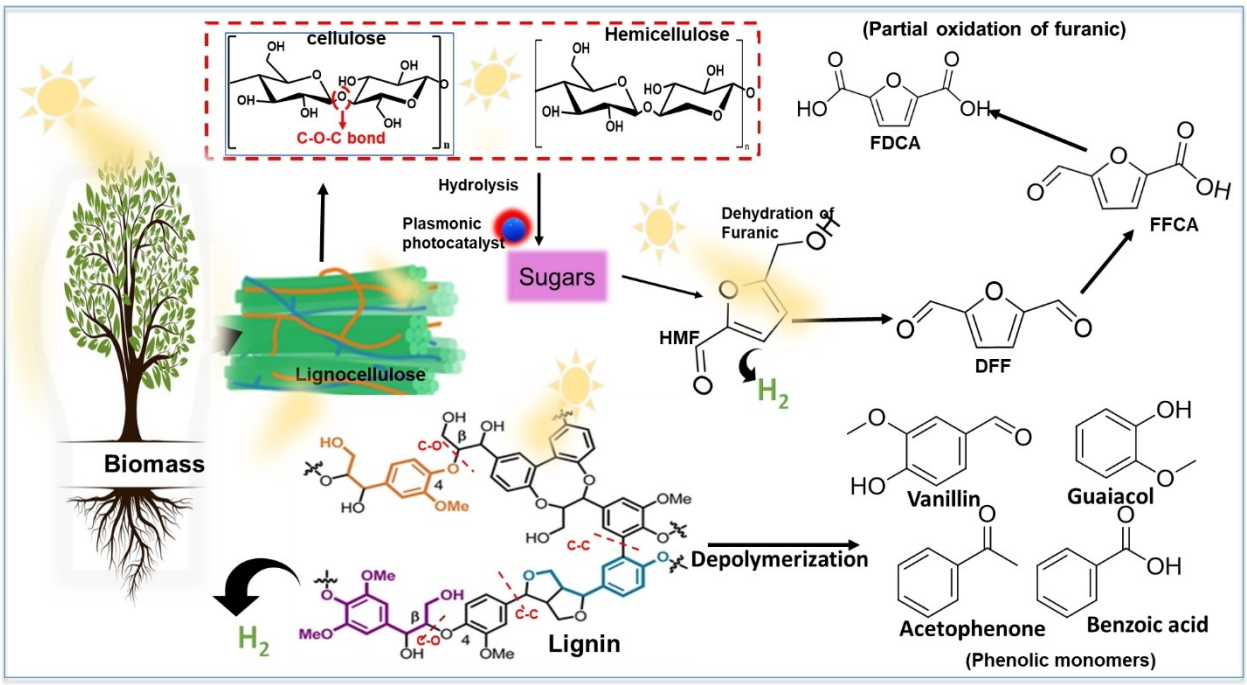

Figure 1. Schematic representation of photocatalytic LCB conversion routes to value-added chemicals and hydrogen gas considered in this review. Note: DFF = 2,5-diformylfuran, FDCA = 2,5-Furandicarboxylic acid, HMF = 5-hydroxymethylfurfural.

conversion. In other words, the photocatalytic oxidation behavior would be different against different types of LCB products. Due to the action of primary ROSs produced, organic substrates form active radical species called radical intermediates, both of which play key roles in biomass conversion. Some key radical intermediates formed on organic substrates include alkoxy radical ($RO^{\bullet}$), hydroperoxide (RO_2H), and peroxy radical ($RO_2^{\bullet}$), which are formed through the activation of various sites of biomass by ROSs.[33,34]

2.2. Photocatalytic biomass conversion to key phenolic aromatic building blocks and mechanistic insights

2.2.1. TiO_2-based photocatalytic conversion of lignin and standing challenges

Compared to other LCB fractions, lignin is the richest aromatic polymer, made of monolignol (guaiacyl, syringyl and p-hydroxyphenyl alcohols) resulting in C–C and C–O bonds with units such as alkyl-alkyl, alkyl-aryl and aryl-aryl interlinkages.[35] Industrially, the isolation of lignin is achieved through three key techniques, thus sulfite process, kraft process and soda process, with kraft lignin being the dominant approach.[36] Among different linkages in lignin, β-O-4 constitutes the most frequent motif with the abundance varying from 43 % to 65 % in natural lignocellulosic LCB.[37] Generally, different variety of photocatalysts, including semiconductors, carbon-based materials, metal sulfides, and organometallic materials, among others have been applied for photocatalytic LCB conversion. Still, TiO_2-based photocatalysts have received the highest attention as a photocatalyst for biomass conversion. The significant use of TiO_2 photocatalyst could be credited to the ubiquitous existence of this catalyst, its stability, low toxicity, and low cost.[19,38] The choice of LCB or fraction of biomass could also determine the product stream. Table 1 summarizes some reports on the use of photocatalysis for biomass conversion to high-value aromatic platform compounds.

From Table 1, photocatalytic conversion of biomass to aromatics has predominantly been achieved through the use of lignin. The use of TiO_2 as a standalone photocatalyst has received significant attention. Due to its large band gap (3.2 eV), TiO_2 only utilizes about 5 % of solar light, thus operating under UV conditions, when used. Also, for studies targeting phenolic-based monomers as products, TiO_2 standalone systems result in product overoxidation and low selectivity. In a typical scenario, the first TiO_2 photocatalyst study using lignin as substrate in water resulted in complete degradation to CO_2.[47] Since then, the scientific community has developed several strategies including doping with metals and non-metals, and other surface modifications to enhance TiO_2 for biomass conversion.[42,44] Srisasiwimon et al.[42] recorded close to 40 % conversion of lignin and other formation of aromatics when a ball-milled TiO_2/Lignin composite mixture was used for photo-conversion of lignin under UVA conditions. The generation of co-radicals such

Table 1: Selected reports of photocatalytic conversion of lignin to value-added chemicals.

No	Biomass source	Photocatalyst	Solvent	Light source	Reaction condition (atm, temp, time)	Product	Conv. [%]	Yield [%]	Ref.
1	Lignin from alfalfa black liquor	TiO_2	H_2O	UV light	r.t, n.d, 0.7 h	coniferylic alcohol, syringaldehyde, vanillin, Catechol, vanillic acid, etc.	n.d	n.d	[39]
2	Lignosulfonate	TiO_2	Sodium acetate buffer	UV lamp	r.t, n.d, 1 h	Guaiacol	n.d	8.7	[40]
3	Lignosulfonate	Bi1 %/Pt1 %−TiO_2	H_2O	300 W Xenon lamp	r.t, n.d, 1 h	Guaiacol	84.5	22.7	[40]
4	Lignin	TiO_2/Lacasse/H_2O_2	Sodium acetate buffer	UV irradiation	50 °C, n.d, 24 h	Organic acid Fatty acid Carbohydrates	100	nd	[41]
5	Kraft lignin	TiO_2/Lignin	MeCN/H_2O	UVA light	r.t, n.d, 5 h	Vanillin	40.3	1.72	[42]
6	Kraft lignin	TiO_2	0.5 M NaOH solution	UV lamp		Vanillin Vanillic acid	92	nd	[43]
7	1 : 1w/w ligninTiO$_2$ ball milled mixtures	1 : 1 w/w ligninTiO$_2$ ball milled mixtures	H_2O	125 W High pressure mercury light	r.t, n.d, 6 h	Ethyl benzene, vanillin, acetovanillone, acetosyringone, syringaldehyde	n.d	n.d	[44]
8	Kraft lignin	TiO_2/H_2O_2	CH_3OH/H_2O	UV/Visible	r.t, n.d, 3 h	Succinic acid	nd	7.8	[45]
9	Rice husk	TiO_2/H_2O_2	H_2O	UV light	r.t, n.d, ≈4.2 h	170 different organic species	n.d	n.d	[46]

as •OH and $•O_2^-$, together with enhanced contact facilitated effective cleavage as revealed by the mechanistic study.

Aside from improving contact, TiO_2 and AgCl nanoparticles were synthesized and used for the full photoconversion of rice husk into over 170 different compounds including phenolic monomers.[48] Mechanistic insights revealed that depolymerization occurred via the development of new energy levels and increased free electrons formed via the migration from the Fermi level of Ag to the TiO_2-based photocatalyst. The promotional effect of this type of substitution has also been revealed elsewhere.[49] Bi and Pt as co-catalysts with TiO_2 (Bi/Pt–TiO_2) have also shown promising results for photo-conversion of lignosulfonate lignin to value-added compounds.[40] Consequently, the designed catalytic system afforded about 84.5 % conversion of lignin and 22.7 % yield of guaiacol with other products such as 4-phenyl-1-buten-4-ol, vanillin, and vanillic acid. The Bi/Pt–TiO_2 catalyst performed better than the singly modified catalyst (Pt–TiO_2 and Bi–TiO_2). The presence of Pt and Bi provided the active sites on TiO_2 which enhanced less oxidative radical species ($O_2^{•-}$), thereby suppressing the formation of highly oxidative radicals such as •OH. Other modified catalysts such as metal sulfides have also been applied for LCB conversion to aromatic compounds. Binary photocatalysts such as (CdS and ZnS) and multi-sulfides ($Zn_mIn_2S_{m+3}$ and $Zn_{1-x}Cd_xS$ and) are examples of modified sulfide-based photocatalysts. With a band gap of 2.4 eV and >520 nm visible light responsiveness, CdS is the most studied metal sulfide for biomass conversion.[50] The conversion of different lignin model compounds was tested over a CdS photocatalytic system and compared with a 1-dimensional CdS@TiO_2 system by Liu et al.[51] The study clearly showed that the 1D CdS@TiO_2 showed higher conversion than using 1D CdS nanowire catalyst only. This was ascribed to the high formation of photoinduced electrons and O_2• in the 1D CdS@TiO_2 system as the key factor leading to high performance than 1D CdS.

Multiple radical co-mediated depolymerization of lignin has gained particular attention. For instance, Ko et al.[52] innovatively developed a 3D compartment photo-electro-biochemical system for lignin depolymerization using TiO_2 as a photocatalyst, an electrocatalyst, horseradish peroxidase and lignin peroxidase isozyme H8 as biocatalyst (Figure 2). The photo-electro-biocatalytic design enabled successful cleavage of β-O-4 linkages in lignin dimers (coniferyl alcohol) via the action of •OH and O_2•. Mechanistically, the coupled photo-electrocatalytic system enhanced the in situ generation of H_2O_2, which was then used by peroxidase isozyme H8 to depolymerize lignin and convert it to high-value monomers.

Also, the oxidation of lignin was undertaken using a synergetic photocatalytic electrocatalytic (also known as photo-electrocatalytic) strategy where Ta_2O_5–IrO_2 and TiO_2–NT were adopted as the electrocatalysts and photocatalyst, respectively.[53] Interestingly, not only did this strategy suppress electron-hole recombination but also the addition of electrocatalytic oxidation, enhanced multiple radical formations than the treatment alone system, leading to the production of vanillin and vanillic acid. To this effect, photo-electrocatalytic coupling strategies could significantly pave the way for enhancing performance with the use of TiO_2-photocatalyst for biomass conversion. As highlighted, photocatalysis promotes polymeric lignin depolymerization to various aromatic compounds and this has predominantly been achieved via the generation of radicals such as •OH and $•O_2$. However, these radicals result in uncontrollable oxidation, which could lead to the mineralization of products. Limiting the mineralization of products in oxidation reactions has become an important but challenging task, making selective oxidation a hotspot area of research. Moreover, selective oxidation can also minimize the additional cost of separating targeted products in reaction media, where various side reactions result in the formation of different products.

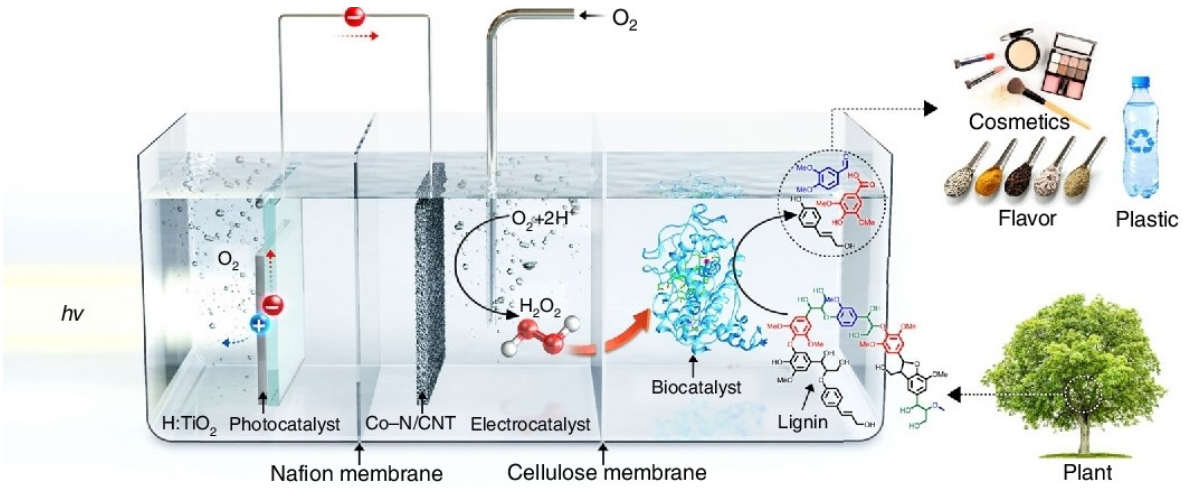

Figure 2. Coupled three-compartment photo-electro-biochemical reactor for lignin depolymerization [Reprinted with copyright obtained from ref. [52]].

2.2.2. Mechanistic insights and strategies for enabling selective activation and cleavage of C_β–O or C_α–C_β linkages to aromatic compounds

Multiple strategies have been adopted to develop novel catalytic systems for the selective oxidation of both C_β–O and C_α–C_β bonds in lignin. Photocatalysis activation and fragmentation of organic substrates occur via common mechanisms such as (i) energy transfer (ii) photoredox catalysis (iii) light-induced transfer of atoms, and (iv) organometallic excitation.[20,28,29] Due to their economic advantage, the use of reduction and oxidation via photoredox reactions has gained significant attention, rather than oxidative half-cell reactions (reduction or oxidation). Organometallic and other molecular-based complexes are widely harnessed in recent years due to their unique ability to form excited state species possessing redox-neutral(reduction and oxidation) characteristics.[20,54] Here, we reviewed the current photocatalytic strategies for enhancing the selective oxidation of lignin to chemicals via the generation of specific radical intermediates and their interaction with ROSs.

2.2.2.1. Redox neutral photocatalytic strategies for cleaving C_β–O linkages

The depolymerization of C–O bonds in lignin could be achieved through one-step or two-step redox-neutral photocatalytic (here after called photoredox) reactions. The two-step fragmentation involves the pre-oxidation of lignin via dehydrogenation of C_α-position (C_αH–OH) to alkoxy intermediate (C_α=O) followed by a photocatalytic reduction step involving the cleavage of β-O-4 linkage in C_β–O under visible light by photogenerated electrons achieved either directly or indirectly to reduce the bond dissociation energy (BDE). The two-step technique was first reported by Stephenson and co-workers[55] in which [4-AcNH-TEMPO]BF_4 was used for the pre-oxidation step followed by photochemical reductive cleavage of β-O-4 linkage (Scheme 1a). The initial step could be done using electrocatalytic, photocatalytic or thermocatalytic strategies.[56,57] Relying on their earlier study, Stephenson and colleagues[58] successfully replaced the pre-oxidation step with a photoredox catalyst [Ir{dF(CF_3)ppy}$_2$(dtbbpy)] and Pd(OAC)$_2$ as co-catalyst in the presence of $Na_2S_2O_8$ and this afforded excellent conversion of different model substrates (Scheme 1a). Consequently, the co-catalytic system promoted a single electron transfer (SET), which initiated a C_α-oxidation to weaken adjacent bonds. Luminescence quenching experiments mechanistically showed that, under visible light conditions, there is the formation of photoexcited Ir ($E_{1/2}$ $Ir^{3+}*/Ir^{2+} = +1.21$ V) occurring via a ligand-metal-charge transfer (LMCT) mechanism. Subsequently, the formed $Ir^{3+}*/Ir^{2+}$ gained an electron from an amine group, making the formed $Ir^{3+}*/Ir^{2+}$ a strong oxidant that can facilitate the activation and cleavage of C–O bonds as depicted in Scheme 1b. Hao and colleagues[59] innovatively immobilized [Ir{dF(CF_3)ppy}$_2$(dtbbpy)] onto a mesoporous cellular silica foam via a thio-lene click reaction thus a vinyl-tagged [Ir(ppy)$_2$(bpy)]PF_6 complex and thiol-functionalized mesoporous cellular silica foams to perform their photocatalytic reaction. Their approach resulted in a heterogeneous type of photocatalyst with a good ability to undertake reductive cleavage of C_β-O bonds available in β-O-4 lignin dimer under visible light.

Notwithstanding this progress, a major challenge associated with the two-step process is the separation of obtained products from the pre-oxidation reaction for the next step. An innovative approach involving a one-step process has been developed. Luo et al.[60] intriguingly elucidated a novel one-pot strategy for enhancing photocatalytic depolymerization via dual-wavelength switching (455 nm and 365 nm) in the presence of two catalysts (Scheme 1c). Under visible light irradiation(455 nm), the Pd/$ZnIn_2S_4$ catalyst can aerobically activate C_α–OH bonds to C_α=O; then the TiO_2–NaOAc system is utilized to cleave C–O bonds in the alkoxy intermediate by a hydrogenolysis reaction under 365 nm light. Interestingly, the dual light wavelength switching approach via an oxidation-hydrogenolysis tandem process resulted in the selective oxidation of ketones and phenols (90 % and 93 %, respectively). Meanwhile, the system generated Ti^{3+}, which was responsible for the photocatalytic-hydrogenolysis of C–O bonds in lignin, according to detailed mechanistic investigations presented in Scheme 1c.

Compared to the two-step process, one-step conversion of C_β–O could be an energy-saving (no need for a further separation/purification of ketone-related intermediates) approach to two-step processes. The one-pot process relies on the design of redox-neutral photocatalytic systems to achieve the activation and cleavage of bonds in a single reaction pot. Wang and colleagues[61] discovered a self-transfer hydrogenolysis protocol using $ZnIn_2S_4$ photocatalyst under visible light to successfully activate and cleave C_β–O bonds of β-O-4 lignin models when exposed to blue LED light. By applying this protocol for organosolv-extracted poplar wood lignin depolymerization, a 10 % yield of *p*-hydroxyl acetophenone derivatives was obtained. According to the mechanistic study, the cleavage of the monomers was achieved via a "hydrogen pool" formed via the $ZnIn_2S_4$ promoted surface dehydrogenation of C_αH–OH groups available in lignin to alkoxy radical intermediate, after which the adjacent C_β–O is cleaved via a hydrogenolysis process. The occurrence of both dehydrogenation/hydrogenolysis in an integrated system depicts a one-pot reaction. Han et al.[62] innovatively controlled reaction product formation by adopting a similar self-hydrogenation approach for the cleavage of a β-O-4 model lignin dimer over Ni/CdS nanosheet. With MeCN as solvent under visible light (440–460 nm) irradiation, the Ni/CdS system enhanced the conversion of 2-phenoxy-1-phenyl ethanol (PP-ol) conversion to 2-phenoxy-1-phenylethanone (PP-one) with H_2 as a product. However, after adjusting the reaction pH with KOH (MeCN/0.1 M KOH = 2/8) the cleavage of C_β–O led to the formation of acetophenone and PP-one as products. The adsorption of protons resulted in reductive cleavage of C_β–O instead of the production of H_2. Wu et al.[45] practically showed a lignin-first biorefining approach (depolymerization

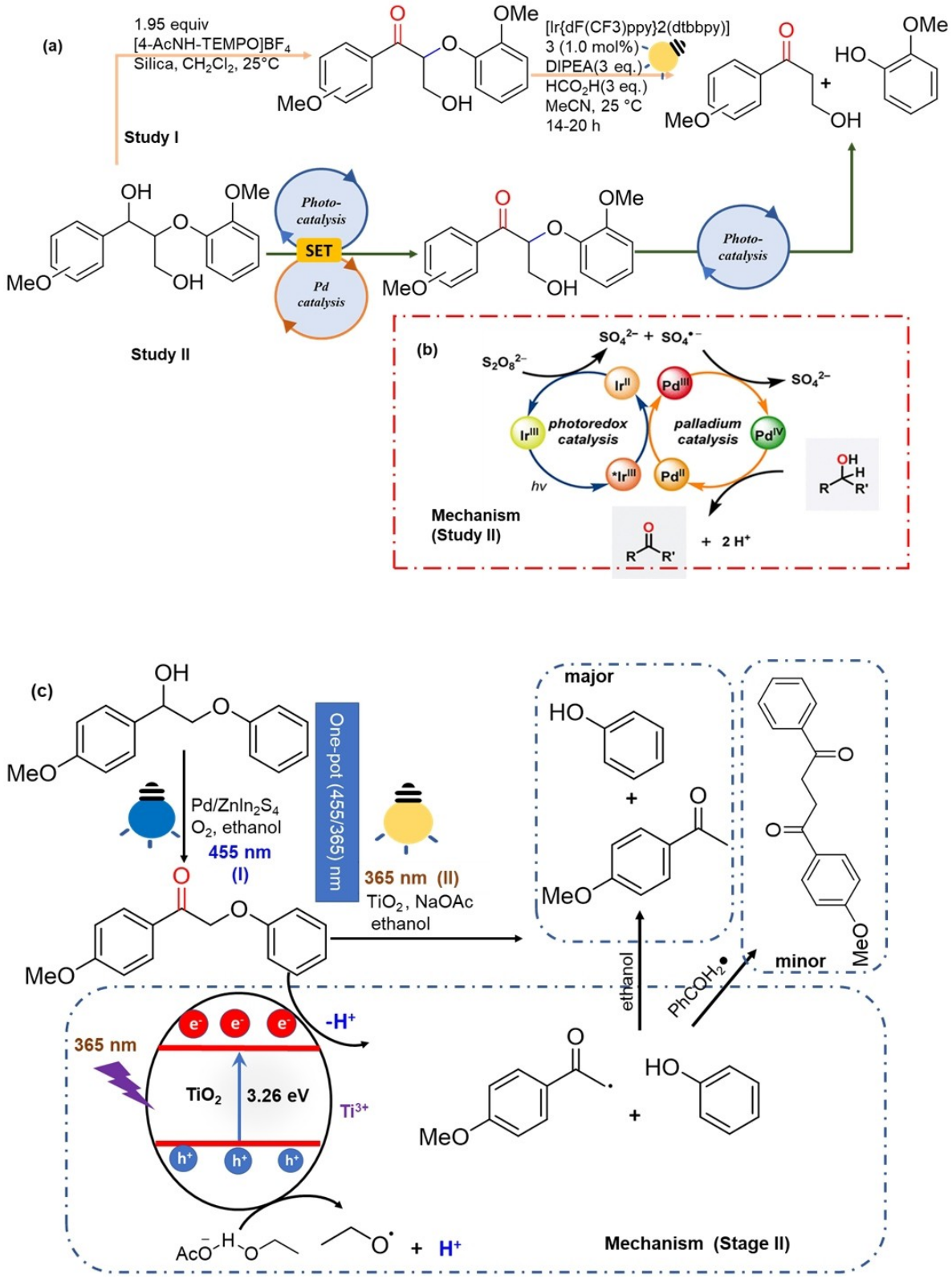

Scheme 1. Strategies for selective cleavage of C–O bonds in lignin and model lignin a) C_α oxidation via a [4-AcNH-TEMPO]BF_4 with subsequent a photochemical reductive cleavage of β-O-4 linkage (Study I).[55] b) A chemoselective approach merging Pd catalysis and a photoredox catalyst, and mechanistic studies (Study II).[58] c) One-pot depolymerization of β-O-4 alcohols into ketones and phenols by oxidation hydrogenolysis reaction via dual light wavelength (455 nm and 365 nm) switching strategy.[60] Schemes 1a, b, and c are reprinted with permission from the American Chemical Society, in 2013 and 2016.

of native lignin in the first step before polysaccharide fraction[12]) via the identification of a novel one-pot C_β–O electron-hole coupled (EHCO) mechanism for the cleavage of C–O bond using a catalyst with tunable redox ability, thus CdS Quantum dots (QDs), and 3-mercaptopropionic acid as ligand. Through a Cα-radical intermediate, electrons & holes successfully cleaved the β-O-4 in PPol affording the yield of phenol and acetophenone under visible light irradiation (Figure 3a). Upon further accepting an electron, the Cα-radical enabled facile cleavage of the markedly weakened C_β–O bonds in the lignin model compound (PP-ol). The CdS QD-4.4 nm efficiently catalyzed the full conversion of native biomass where about 27 wt % functionalized aromatics monomers were obtained under solar light (Figure 3b). The proposed protocol depicted a lignin-first strategy with high retention of polysaccharide fraction after photocatalysis (Figure 3c) which was taken via further acidolysis and enzymatic hydrolysis (Figure 3d).

2.2.2.2. Photocatalysis methods for precise cleavage of C_α–C_β bond in model and native lignin

One main reason why lignin remains recalcitrant to being depolymerized to high-valued monomers is the prevalence of C_α–C_β crosslinked structures. Conventional approaches for C_α–C_β bond cleavage have been targeted, but they are typically robust, unselective, promote product repolymerization, and the need for numerous reaction steps which make them unattractive for integrating into existing biorefineries.[12]

While the cleavage of C_β–O bonds in β-O-4 may occur through the activation of C_αH–OH to alkoxy intermediates and subsequent cleavage of adjacent C_β–O bonds during lignin depolymerization, the bond dissociation of C_α–C_β bonds increases under robust reactions. More interestingly, the development of photocatalytic conversion of β-1 and β-O-4 bonds in lignin could rapidly provide important routes for depolymerizing C_α–C_β bonds. One way to enhance C_α–C_β bond in β-1 model lignin is via through the activation of C_β–H to key intermediate radicals.[63] Most importantly, a highly selective photocatalyst for oxidizing β-1 and in C–C linkages should preferentially activate the C_β–H bond while limiting the production of ketones due to a possible increase in bond dissociation energy (Scheme 2).

Hou et al.[64] prepared a heterogeneous photocatalyst $CuO_x/CeO_2/TiO_2$ nanotube hybrid for selective oxidation of C_α–C_β bonds under visible light irradiation (Scheme 3a). The selectivity of this photocatalyst towards benzaldehyde production from 1,2-diphenylethanone was approximately 99 % with 1 % diphenylethanone. However, when TiO_2 alone was used under UV-light (365 nm), the product selectivity dropped significantly to 16 %, respectively. Similarly, Liu and colleagues[65] explored the possible cleavage of 2-phenoxy-1-phenylethanol (contains C_α–C_β, C_α–OH, and C_β–O bonds) using TiO_2-Anatase, TiO_2 P_{25}, and Bi_2WO_6 and g-C_3N_4. However, TiO_2-based photocatalysts showed little performance towards the cleavage of C_α–C_β, as compared to the other photocatalysts. Indicating that the use of commercially available TiO_2 alone as a photocatalyst for the cleavage of C–C bonds has not been successful.

Recently, the use of graphene-based photocatalysts catalyst is deeply explored due to their narrow band gap and visible light photoresponsiveness. Liu et al.[65] used mesoporous g-C_3N_4 to cleave both C_α–C_β of β-1[1,2-diphenylethanol (−1 model)] and β-O-4 model (PP-ol), under visible light irradiation(455 nm) (Scheme 3b). Both benzoic acid and benzaldehyde were major products obtained with a total yield between 66–90 %. The enhanced performance as revealed by the mechanistic investigations showed the formation of C_β-radical intermediates, thereby promoting the activation of C_β–H bond (Scheme 3b). Hence, the activation of C_β–H bond remains a critical step for the cleavage of C_α–C_β bonds. Meanwhile, the existence of π–π stacking interactions between the lignin model compounds and the surface of the mesoporous g-C_3N_4 formed via the adjustment of nitrogen group in g-C_3N_4 promoted the activation/deprotonation of PP-ol to radical intermediate before cleavage of C_α–C_β bonds. This phenomenon was also revealed in the study by Du et al.[66]

Over the past decade, homogeneous photocatalysts such as metal complexes (e.g. iridium-based complexes) have been used to facilitate the activation and fragmentation of C_α–C_β bonds in biomass. Nguyen et al.[67] used an Ir-based

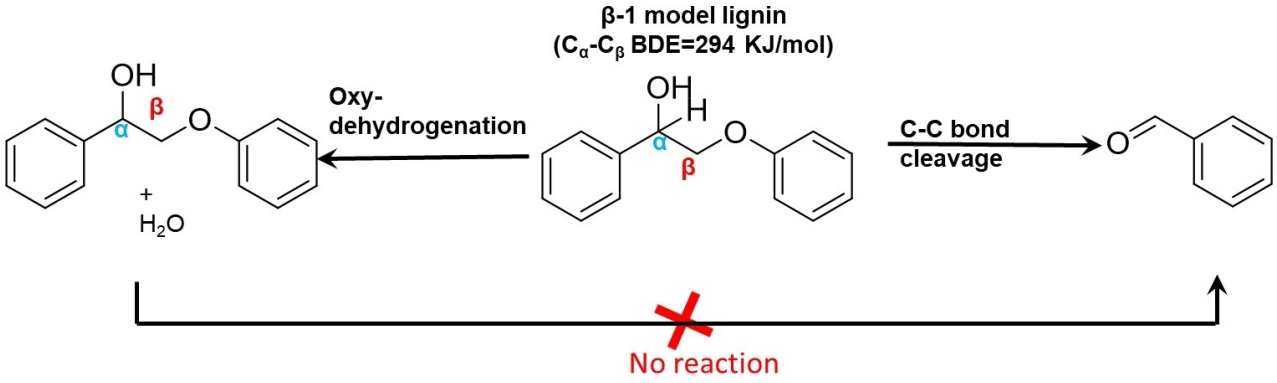

Scheme 2. Cleavage of C_α–C_β via C_β–H activation vs oxy-dehydrogenation routes.[63,64] Adapted with permission from Angewandte Chemie - International Edition and American Chemical Society.

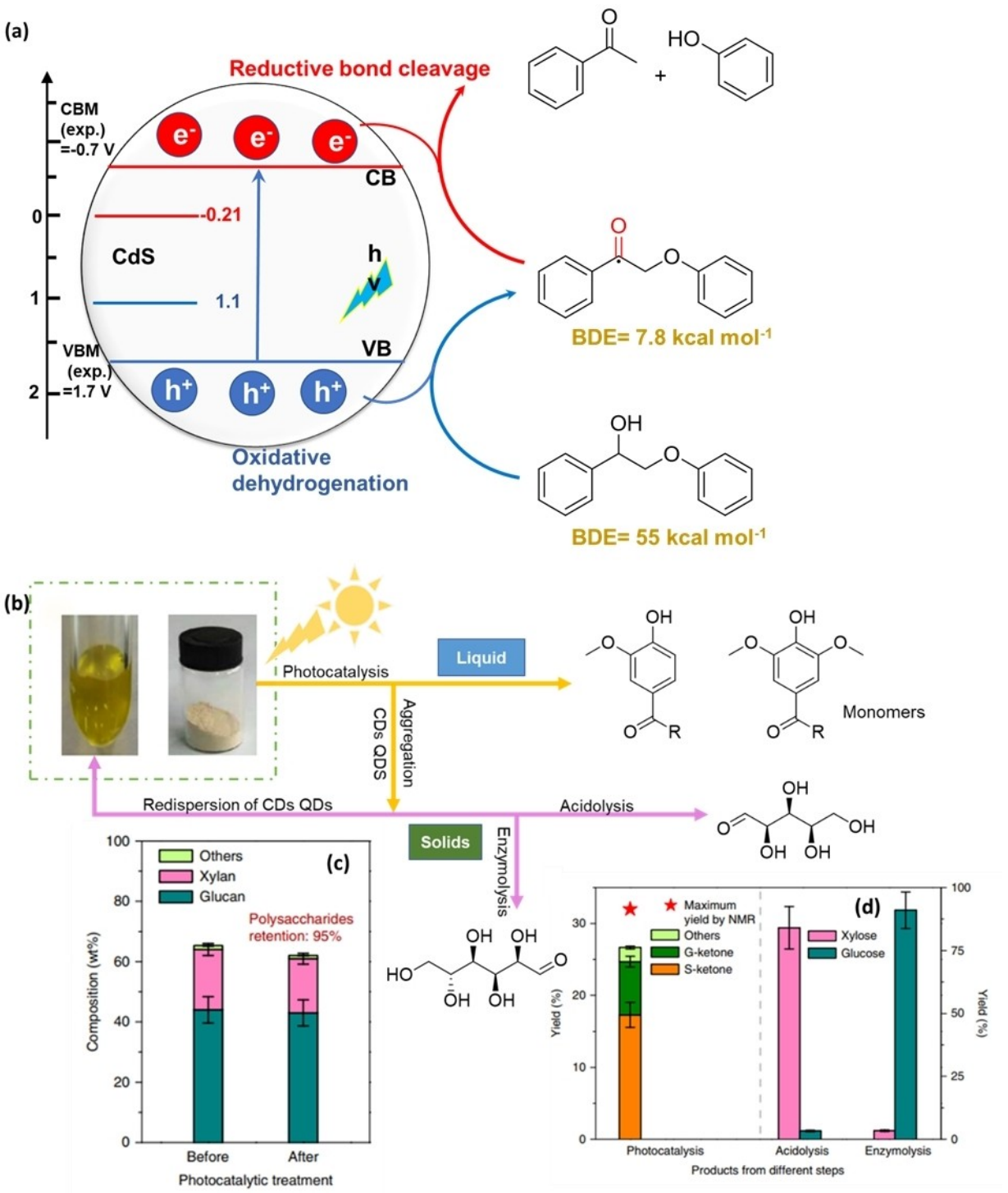

Figure 3. Photocatalytic full lignocellulosic biomass conversion in a lignin-first approach.[45] a) Proposed mechanisti insight into the cleavage of dimeric β-O-4 bonds in PP-ol over CdS QDs via C_α-radical intermediate produced from a photoredox electron-hole coupled (EHCO) strategy. b) Schematic representation of lignin-first depolymerization of lignin under solar light, product yields, and catalyst recycling c) Polysaccharide retention before and after photocatalysis. d) Product yields from acidolysis and enzymolysis of polysaccharides. Reproduced with permission from Springer-Nature copyright 2018.

complex in a photoredox reaction under visible light to promote a proton-coupled-electron-transfer (PCET) process that enabled O–H activation to form alkoxy radical intermediates. Alkoxy radical intermediates have unique reactivity patterns (C–C bond scission and hydrogen atom transfer) and they could easily be cleaved.[22] Hence, the PCET technique's formation of alkoxy radicals intermedi-

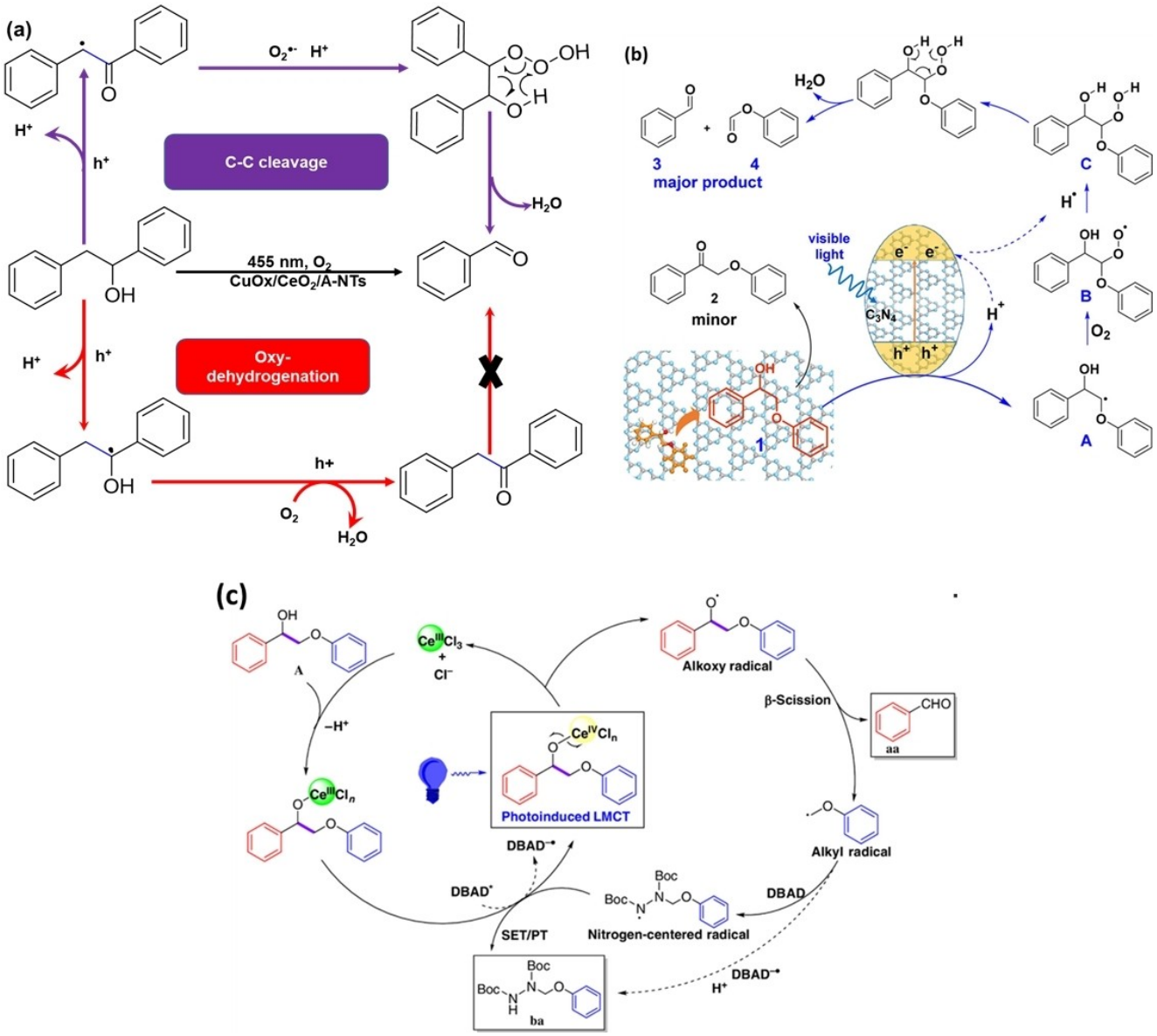

Scheme 3. Novel strategies for C_α–C_β bond cleavage in lignin models. a) The mechanism for CuO_x/ceria/TiO_2 promoted cleavage of C_α–C_β in β-1 linkage via C_α-radical attack.[64] b) The mechanism for UV/Visible mesoporous g-C_3N_4 catalyzed the transformation of PP-ol.[65] c) $CeCl_3$ photocatalytic cleavage via a photo-induced ligand-to-metal-charge transfer (LMCT).[68] Note: Schemes a and b are adapted with permission from the American Chemical Society and c is from Chinese Chemical Society Journal.

ates successfully cleaved C_α–C_β bonds, yielding 96 % phenylethers and 97 % benzaldehydes.

The controlled initiation of the PCET process has been reported to also facilitate the formation of superoxides from C_β–H bond activation to enhance bond cleavage in the model and native lignin. Bosque et al.[56] creatively designed a potential-controlled system with N-hydroxyphthalimide/2,6-lutidine-electrocatalyst for hydrogen atom transfer (HAT) and $Ir(ppy)_2(dtbbpy)]PF_6$/diisopropylethylamine (DIPEA) as a photocatalyst. The formation of two superoxides per each fragmentation occurring via the PCET mechanism enhanced performance. Consequently, simultaneous cleavage of C–O/C–C in pine native lignin was achieved via one electron transfer and two protons, affording two products of 1.30 and 1.14 wt %. The same group also proposed a photoredox PCET strategy where the formation of alkoxy radical intermediate successfully enabled the cleavage of C–C bonds in native lignin, which afforded the formation of vanillin and 4-(2-hydroxyethoxy)-3-methoxybenzaldehyde yields of 2.4 and 1.6 wt %, respectively.

Notwithstanding this progress, organometallic catalysts used for precise control of radical formation are generally sensitive to reaction conditions, tolerant to selected functional groups, and could deactivate complicated conditions for biomass conversion environments. Wang and colleague[68] adopted a one-pot strategy for the depolymerizing and amination of C–C bonds in lignin using $CeCl_3$ as a photocatalyst and designed a protocol involving the inter-

mittent switching on and off of the external visible light. By applying this protocol to model lignin, aldehyde (up to 97 %) and nitrogen-containing products (up to 95 %) were obtained from the cleavage of the C_α–C_β bond available in β-1 models (Scheme 3c). Mechanistically, the creation of $Ce^{III}Cl_n$/lignin complex via the deprotonation of the α-OH group and subsequent oxidation of $Ce^{III}Cl_n$/lignin to $Ce^{IV}Cl_n$/lignin and via the ligand-to-metal charge transfer (LMCT), homolysis oxidation of $Ce^{III}Cl_n$/lignin led to the formation of both alkoxy radical intermediates and the nitrogen-centered radical intermediate. The photoproduced ROSs successfully enhanced yield even in native lignin. This method impressively depolymerized native pine lignin, generating 11.94 wt % aromatic platform chemicals. It is important to note that, the alkoxy radical intermediate could be quenched/controlled if it reacts with oxygen or hydrogen donor to form ether and formate, respectively.[69,70]

2.2.3. Summarized strategies for controlling the formation of radical intermediates in lignin

Due to the high reactivity of most active radicals produced during photocatalysis, a critical step in the photocatalytic downstream conversion of biomass is the development of strategic approaches for regulating active radical species such as photo-activated molecular oxygen and substrate-derived radical intermediates. The abundance of O–H groups in lignin enables precise activation of O–H bonds to alkoxy radical intermediates which can further weaken adjacent C_α–C_β or C–O bonds, and this unique protocol has been used in the lignin depolymerization process. To regulate the formation of alkoxy radical intermediates in photocatalytic biomass conversion, novel photocatalytic strategies have been developed with novel reaction mechanisms. Table 2 and Figure 4 summarize the typical catalysts and mechanisms which regulate the formation of C_α-radical intermediates (alternatively called alkoxy radical intermediates) during the cleavage of C_α–C_β and C–O in *β*-O-4 and *β*-1 model lignin substrates.

Overall, the activation/pre-oxidation and fragmentation of C–O bonds in lignin have been promoted using various photocatalytic processes, ranging from reductive (electrons/reducing agents), oxidative process (holes/oxidizing agents), and redox neutral processes (holes and electrons). As summarized in Table 2, different homogeneous and heterogeneous-based photocatalysts have been applied for regulating the formation of this intermediate. Homogenous photocatalysts, such as organometallic complexes (Ir-, and vanadium-based) have been adopted due to high tunable properties and are generally selective towards the cleavage of C_α–C_β and C–O bonds in lignin. Strategies such as changing ligands, co-catalyst, or types of metals have been used to tune these homogeneous photocatalysts. The pre-oxidation step has also been achieved using metal-free catalysts such as N-hydroxyphthalimide and ionic liquids.[50,73] However, the choice of this catalyst is mostly advised if separation problems can be solved. Aside from homogeneous photocatalysts, heterogeneous photocatalysts are also predominantly applied for the conversion of C_α–C_β and C_β–O bonds. As summarized in Table 2 and preceding sections, photocatalysts such as metal sulfides (e.g. CdS, In_2S_3, etc.), carbon-based photocatalysts(e.g. g-C_3N_4), hybridized forms, among others are being adopted for such photon-induced biomass conversion. The application of metal sulfides for biomass conversion has also been

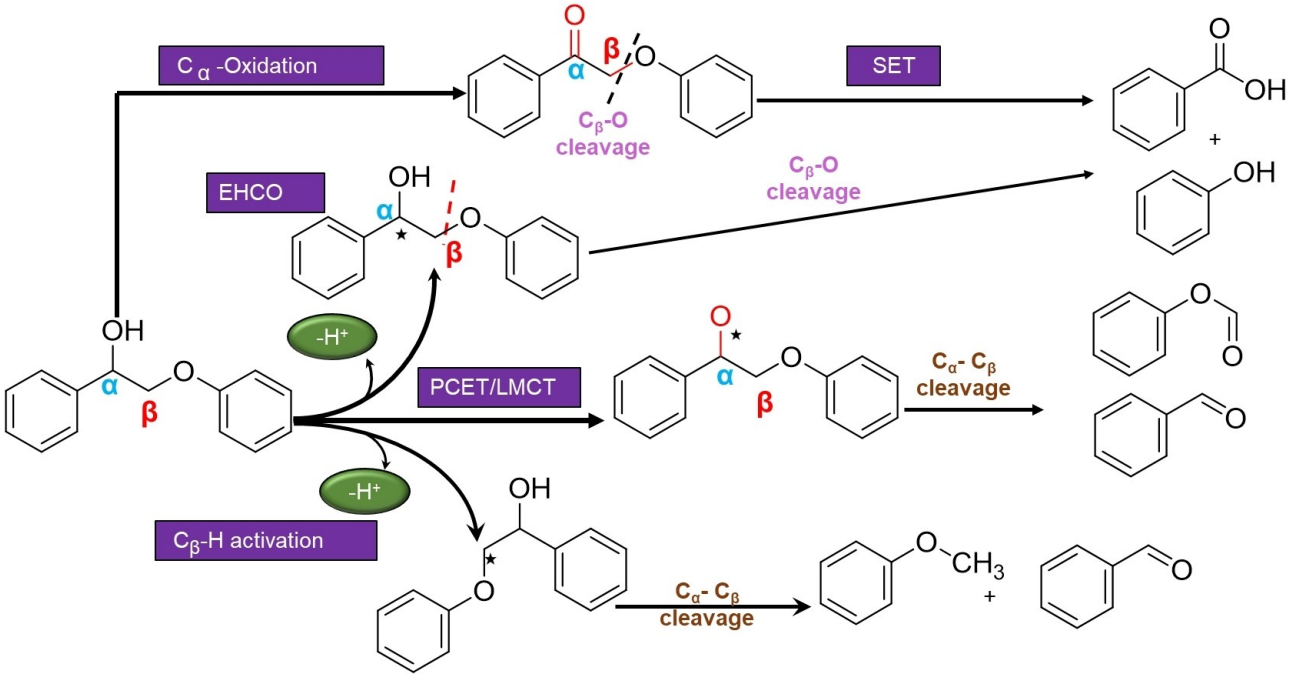

Figure 4. Summary of key mechanisms for C_α–C_β and C–O bond cleavage via photocatalytic lignin activation and depolymerization.

Table 2: Summarized strategies for regulating/controlling the formation of radical intermediates in model lignin.

Selective bond scission	Substrate	Mechanism for activating O–H bonds to Cα- radical intermediates	Photocatalyst (Wavelength)	Product	Ref
C_α–C_β in β-O-4 models	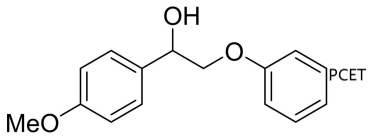	PCET	[Ir(dF(CF3)ppy)2(5,5′(CF3)dpy)](PF6 (*50 W blue LED light*)	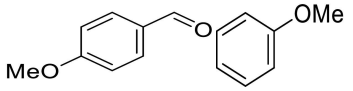 Y: 93% Y = 94%	[70]
	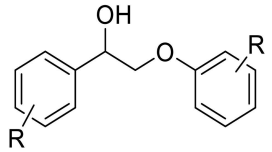	SET and LMCT	$[Ir[dF(CF_3)ppy]_2(dtbbpy)]PF6/Na_2S_2O_8/Pd(OAc)_2$ (*visible light*)	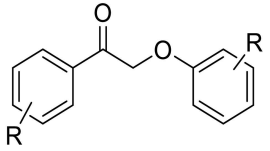 Y: > 99% C: 96%	[58]
	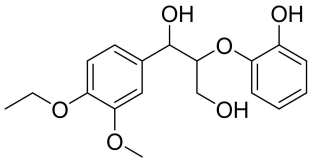	LMCT	Vanadium oxo complexes (*visible light > 420 nm*)	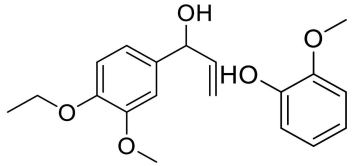	[71]
	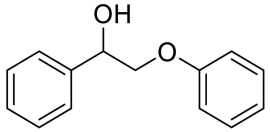	π–π stacking activates to β-phenoxy radical intermediates	$g\text{-}C_3N_4$ (*Visible light > 420 nm*)	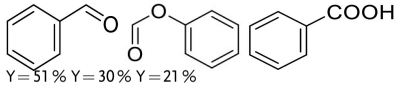 Y = 51% Y = 30% Y = 21%	[65]
	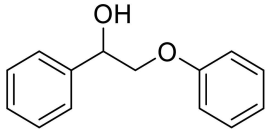	LMCT	$CeCl_3$/DBAD/nBu_4NCl (*30-W blue LED*)	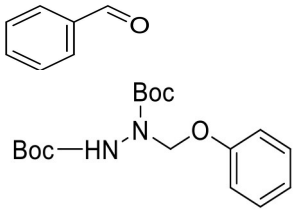 Y = 97% Y = 94%	[68]
C_α–C_β in β-1 models [2]	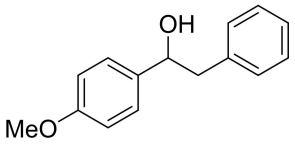	PCET	Ir^{III} photocatalyst $[Ir(dF(CF_3)ppy)_2(5,5'd(CF3)dpy)](PF6$ (*50 W blue LED light*)	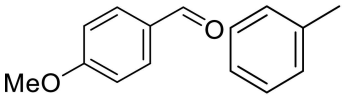 Y = 96% Y = 94%	[70]
	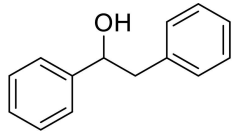	LMCT	$CuO_x/CeO_2/TiO_2$ (*Visible light > 420 nm*)	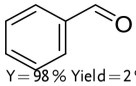 Y = 98% Yield = 2%	[64]

Table 2: (Continued)

Selective bond scission	Substrate	Mechanism for activating O–H bonds to Cα- radical intermediates	Photocatalyst (Wavelength)	Product	Ref
C_β–O in oxidized and pre-oxidised models	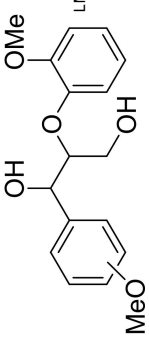	LMCT	[4-AcNH-TEMPO]BF_4/ $[Ir(ppy)_2(dtbbpy)]PF_6$ (*Visible light > 455 nm*)	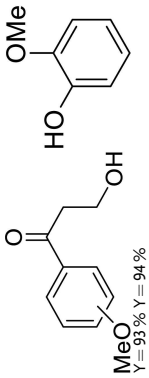 Y = 93 % Y = 94 %	[55]
	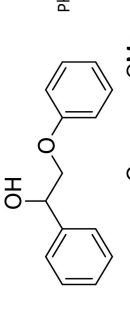	Photoredox EHCO mechanism	Ligand-controlled CdS QDs (*Visible light λ ≥ 400 nm*)	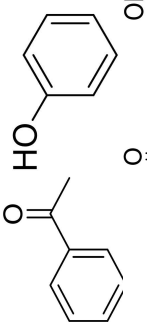	[45]
	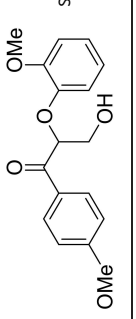	SET mechanism	Perylene diimide (PDI) as a metal-free organocatalyst/HCOOH (*Blue LEDs*)	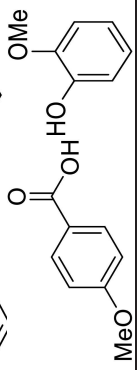	[72]

reviewed elsewhere.[50] The innovative ligand-mediated modification of CdS into soluble QDs for instance by Wu et al.[45] is praised for its outstanding performance towards the cleavage of model and native lignin.

As presented in Table 2 and simplified in Figure 4, the cleavage of C–C bonds in biomass via photocatalytic technique has been mediated by mechanisms such as proton-coupled electron transfer (PCET), ligand-to-metal charge-transfer (LMCT), single-electron transfer(SET), π–π stacking interaction, among others. The SET mechanism combines both radical and ionic reactions which play a key role in organic chemistry. The SET mechanism is usually fast and unstable and has been a target in most lignin depolymerization reactions, especially for the cleavage of C–O bonds. The SET mechanism has been depicted in key lignin depolymerization reactions by Zhang and co-workers[72] involving the use of an organo-photocatalyst perylene diimide (PDI) for the cleavage of C–O bonds. The diisopropylethylamine (DIPEA) oxidant reduces the photo-generated PDI to $PDI^{\bullet-}$ even as the produced $PDI^{\bullet-}$ anion transfer electrons to the lignin/formic acid complex to form a radical intermediate. Consequently, the HCOOH can deprotonate the radical intermediate to enable subsequent C–O bond cleavage. The PCET mechanism promotes the simultaneous transfer of electrons and protons and has been reported to have a kinetic advantage over two-steps SET and HAT reactions.[74] Contrarily to photo-redox reactions, LMCT as an emerging mechanism for activation and cleavage of bonds in biomass does not rely on a link between redox potentials, instead, using the predominantly available metal complexes. Due to this, this mechanism has been targeted to control and improve selectivity in most photocatalytic lignin reactions. Zhang et al.[75] in a review critically provided key routes to utilizing the LMCT mechanism to enhance the visible light responsiveness of commercially available TiO_2, which has so far received little attention in cleaving C_α–C_β bonds in lignin due to its shortcomings in responding to visible light. The detailed understanding of the mechanism and role of key photo-catalyst discussed here should open the door for the development of key strategies to promote the simultaneous activation and cleavage of C–O and C–C bonds in one-pot systems from the mechanistic point of view, which has so far received little attention.

2.3. Dual conversion of polysaccharide-based biomass and derivatives to chemicals and hydrogen gas via photocatalysis

As defined by the US Department of Energy, carbohydrates can be transformed into less functionalized platform chemicals (easy to transform compared with lignin) via the use of different technologies.[76] Polysaccharide-derived chemicals include the scission of glycosidic bonds (C–O–C) bonds to monosaccharide sugars, furanic compounds (including furfural, furfuryl alcohol, HMF and FDCA), organic acids, etc. More specifically, the oxidation of alcohols and aldehydes to carboxylates, the cleavage of C–C interlinkages, and the dehydration of fructose to HMF, and further upgrade of

these products could be achieved using photocatalysis. Also, the conversion of hydroxyl or aldehydes groups in polysaccharides, such as furfural or HMF could produce key bio-based carboxyl or carbonyl products, which are important platforms for furanic-based polymer production or fine chemicals. Table 3 summarizes some applications of photocatalysis for the valorization of polysaccharide-based biomass fractions.

2.3.1. Selective oxidation of monosaccharides and derivatives via plasmonic photocatalysts

Different products have been obtained following the conversion of polysaccharides using photocatalysis (Table 3). The first step for photocatalytic conversion of a polysaccharide to H_2 involves the hydrolysis of β-1,4 glycosidic bonds (C–O–C) to monosaccharides or their intermediates followed by further oxidation of the monosaccharides.[94] Conversion of biomass to H_2 (photo-reforming) with water as a solvent is difficult due to the strict pH demand. Recently Zou and colleagues[78] designed a one-pot strategy for the direct photo-reforming of cellulose. This protocol involved the use of 0.6 M sulphuric acid for the hydrolysis of cellulose to monosaccharides at a temperature of 130 °C over a platinized TiO_2 photocatalyst under UV conditions. Consequently, the concurrent generation of electron donors stimulated direct biomass conversion to glucose, with the products also serving as low oxidative power electron donors. To promote the conversion of polysaccharides to key monosaccharides and their derivatives, photocatalysts have been tuned to achieve a plasmonic thermal effect to enhance the hydrolysis process. This could promote the one-pot conversion of biomass instead of the separate multi-step processes involving pretreatment, hydrolysis, and conversion to useful chemicals. Under visible light conditions, Wang et.[95] successfully cleaved C–O–C β-1,4 glycosidic bonds in cellulose to glucose and HMF, with a zeolite (HY)-based as the acid catalyst and Au-nano particles (designated as Au-HYT) as the plasmonic photothermal catalyst. The study reported a 48.1 % yield of glucose and a 10.6 % yield of HMF at an operating temperature of 140 °C for 16 hours (Figure 5a). The plausible mechanism for photothermal heat production and acid site generation is depicted in (Figure 5b). Firstly, a localized surface plasmon resonance (LSPR) effect on the Au-NPs via light irradiation caused a polarized electric field of the additional cations available in a zeolite (HY) to produce an acid proton (H^+), which attacked the stretched polarized bonds (Step I). More negative oxygen is formed in β-1,4 glycosidic bonds via the continuous stretching of bonds, which leads to the cleavage of C_1–O β-1,4 glycosidic bonds to form glucose together with a carbon cation (Step II). Meanwhile, further hydrolysis of the cation leads to the formation of glucose and a proton (H^+), while HMF is formed from the dehydration of glucose by the zeolite acid catalyst.

A zeolite (Ir/zeolite) photothermal system was designed to cleave C–O–C β-1,4-glycosidic bonds in cellobiose (–a dimeric glucose) and non-pretreated cellulose to monomeric glucose under visible light conditions and temperatures < 100 °C.[96] The Ir/zeolite selectively cleaved C–O–C β-1,4-glycosidic bonds in cellobiose to glucose (> 99 % selectivity). The conversion of non-pretreated crystalline cellulose tested over Ir/zeolite at 90 °C showed 75.3 and 8.4 % of total products (glucose, HMF, and cellobiose) under light and dark conditions, respectively. Under visible light, the active cooperation of Ir as the source of plasmonic photothermal catalyst and HY as an acid catalyst was evident and this followed a similar mechanism described by Wang and colleagues[77] (Figure 5b).

Also, derived monosaccharides such as fructose was converted to HMF using a semiconductor and a Brønsted acid catalytic system under light irradiation.[97] Compared with the metal oxides (WO_3, α-Fe_2O_3, and TiO_2) reaction system, coating the semiconductor with silanol, significantly enhanced the yield of fructose to HMF (yield of 97 %) under visible light conditions andat mild temperature (80◦C) with H_3PO_4 as solvent. Mechanistically, Si via the plasmonic process directly converted the irradiated light to thermal energy, while the prevalence of an O–H group on silanol also triggered high adsorption of fructose via hydrogen bonds. On top of that, the transformation of glucose to organic acids such as glucaric and gluconic acids (used in food, chemical, and pharmaceutical industries) has been achieved using TiO_2-based photocatalysts.[82,98,99] In 2011, Colmenares et al.[82] via an ultrasonication-assisted sol-gel method prepared a structured TiO_2 for photocatalytic conversion of glucose. Their findings afforded gluconic and glucaric acids with selectivity and conversion of > 50 % and 11 %, respectively. They speculated that the lower affinity of gluconic and glucaric acids to the surface of the catalyst reduced the onset of mineralization, hence the high selectivity of products. In 2013, the same group used metal-supported TiO_2 to demonstrate enhanced selectivities toward the yield of gluconic acid and glucaric acids. Thus, doping of Fe^{3+} into the lattice site of TiO_2 via a Fe-doped/TiO_2/zeolite-Y was able to reduce the band gap of TiO_2 (to 2.3 eV), ensuring 94 % the selectivity towards the yield of organic acid (gluconic and glucaric acids).[82] In 2017, an unmodified TiO_2 was first reported to be photoresponsive under visible light conditions and successfully converted glucose conversion.[100] Interestingly, the adsorption of glucose on the surface of TiO_2 promoted a ligand-to-metal charge-transfer effect, thereby enhancing photo-responsiveness under visible light conditions. Overall, a 42 % conversion of glucose was achieved with products such as gluconic acid, glyceraldehyde, erythrose, formic acid, and arabinose. Unfortunately, reactions conducted under UVA conditions showed high product mineralization.

2.3.2. Selective oxidation of furanic and their derivatives

Photocatalysis has been applied for upgrading biomass-derived furanic compounds to key platform alcohols and carboxylic FDCA and DFF.[101] The conversion of furanic and furanic derivatives can be driven via reaction pathways such as dehydrogenation.[102,103] The selectivity of a desired

Table 3: Photocatalytic conversion of polysaccharides and their derivatives into chemicals and fuels.

No.	Biomass	Photocatalyst	Light source	Solvent	Conditions (temp, atm, time)	Product	Yield/Selectivity/Conversion	Ref.
1	Cellulose	Au-HYT	Visible light	H_2O	140 °C, n.d, 16 h	Glucose HMF	S = 48.1 S = 10.6	[77]
2	Cellulose	Pt/TiO_2	Iron doped lamp 250 W	H_2SO_4	130 °C, Ar, 10 h	H_2	Y = 432 μmol h^{-1} g_{cat}^{-1}	[78]
3	Cellulose	TiO_2/Ni–S	Xe lamp 500 W	H_2O	80 °C, N_2, 3 h	H_2 Glucose	Y = 3020 μmol h^{-1} g_{cat}^{-1} n.d	[79]
4	Cellulose	TiO_2/NiO_x@ g-C_3N_4	Xe lamp 500 W	H_2O	80 °C, N_2, 5 h	H_2	Y = 4150 μmol h^{-1} g^{-1}	[80]
5	Cellulose	Pt/TiO_2	UV–A irradiation	H_2O	nd, N_2, 4 h	H_2	Y = 27 μmol h^{-1} g_{cat}^{-1}	[81]
6	Glucose	TiO_2	Mercury lamp	H_2O/ MeCN	r.t., n.d, 10 mins,	Glucaric acid, gluconic acid and arabitol	C = 11 S = 71.3	[82]
7	Glucose	Rh/Rutile TiO_2	Xenon lamp (300 W)	H_2O	r.t, n.d, 4 h	Arabinose and Erythrose	S = 95.3	[83]
8	Glucose	Ru–$LaFeO_3/Fe2O_3$	Visible		rt, n.d, 4 h	H_2	Y = 910 μmol h^{-1} g_{cat}^{-1}	[84]
9	Glucose	Pt/TiO_2 brookite	365 nm	H_2O	r.t, N_2, 7 h	H_2, Arabinose Formic acid erythrose	Y = 242 μmol h^{-1} (0.3–0.8 gL_{cat}^{-1}) C = 77%	[85]
10	Ethanol Glucose Xylose 2-furaldehyde HMF	$AuNPs/TiO_2$	UV light and visible light	H_2O and Na_2CO_3 as additive	30 °C, n.d, 4 h	Acetic acid Gluconic acid Xylose acid 2-furoic acid FDCA	UV C = 98- > 99 S = 90–9 Visible C = 99- > 99 S = 95–99	[86]
11	HMF	P-doped $Zn_xCd_{1-x}S$	LED light source	H_2O	r.t, Ar, 2 h	H_2	S = 65 C = 91 Y = 419 μmol h^{-1} g^{-1}	[87]
12	HMF	TiO_2-m	simulated solar radiation	H_2O	30 °C, O_2, 1 h,	DFF	S = 13 C = 25	[88]
13	HMF	P25	visible light (λ = 515 nm)	MeCN	n.d, O_2, 4 h	DFF	C = 18 S = 69	[89]
14	HMF	SGH–TiO_2 P25	visible light (λ = 515 nm)	MeCN	n.d, O_2, 4 h	DFF	C = 59 S = 87	[89]
15	HMF	metal-free g-C_3N_4	xenon lamp (300 W, $\lambda > 400$ nm)	MeCN and $PhCF_3$	r.t, O_2, 6 h	DFF	C = 31 S = 85.6	[90]
16	HMF	Nb_2O5–800	visible light	$PhCF_3$	r.t, O_2, 6 h	DFF	C = 19.2 S = 90.6	[91]
17	HMF	$MAPbBr_3$	blue LED	MeCN	15 °C, Air, 10 h	DFF	C = 100 S = 90	[92]
18	Furfural alcohol & HMF	Ni/CdS	blue LED	H_2O	r.t, N_2, 8 h	Furoic acid H_2, FDCA	Y = > 90 C = 100	[93]

r.t—room temperature, nd—no data, C.-conversion, S = Selectivity, Y = Yield, FDCA = 2,5-furandicarboxylic acid, DFF = 2,5-diformylfuran, MeCN = Acetonitrile and Au-HYT = H-form Y-zeolites (HY) decorated with Au-NPs.

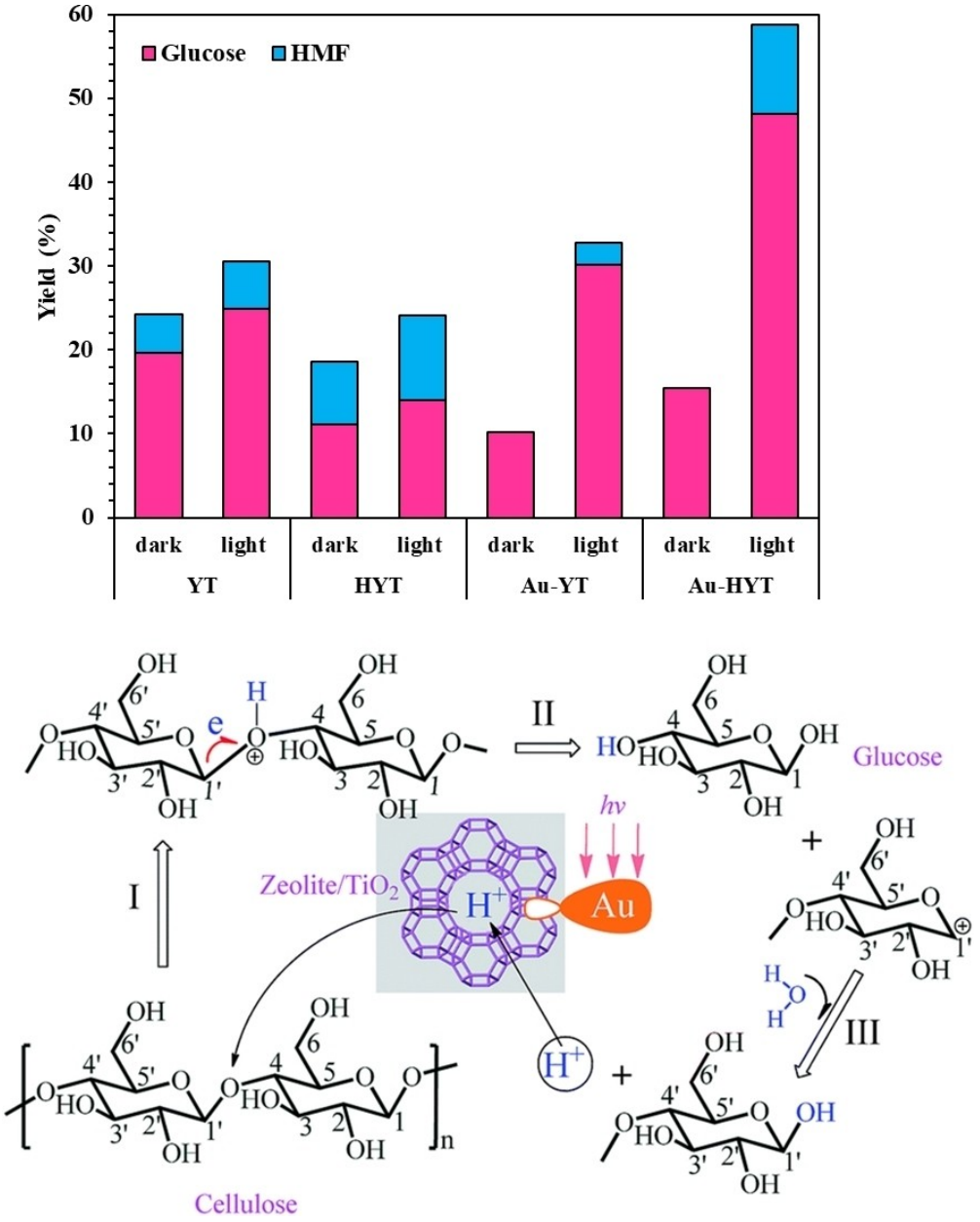

Figure 5. Hydrolysis of C–O–C β-1,4 glycosidic bonds in cellulose to glucose and HMF. a) Au-zeolite composite promotion of cellulose hydrolysis and photo-assisted plasmonic effect mechanism.[77] b) Mechanistic pathway for selective hydrolysis of C–O–C β-1,4 glycosidic bonds to glucose. Adapted with permission from Wang et al.[77]

product relies on the production of specific radical intermediates and ROSs via photocatalytic oxidation or reduction of substrates.

Lolli et al.[103] via a microemulsion method prepared TiO_2 for HMF oxidation, yielding DFF, CO_2, and other products. By introducing Au into the prepared catalysts, the selectivity of DFF was slightly improved. Notwithstanding the slight increase in selectivity, the mineralization of products to CO_2 was significantly high, due to further oxidation of DFF via aliphatic chain intermediates. The selective conversion of HMF to DFF was enhanced by the cooperative interplay of photogenerated charges (h+/e−), the formation of alkoxide radical intermediate and the active role of superoxide ROS.[102,104] Cheng et al.[102] via a photocatalytic approach partially oxidized HMF to DFF using a hydrothermally prepared Bi_2WO_6/mesoporous g-C_3N_4. The 12 % Bi_2WO_6/g-C_3N_4 recorded the highest selectivity and conversion of 84.3 and 59.3 %, respectively after 6 h of photo-irradiation. Mechanistically the high yield was speculated to be initiated by a z-scheme mechanism which promoted electron-hole separation, with $^{\bullet}O_2^-$ being the main ROS, and the formed alkoxide intermediates, successfully enhanced performance. Zhang and co-workers[90] demonstrated the successful conversion of HMF to DFF using a g-C_3N_4 photocatalyst under visible light (Scheme 4). Under visible light conditions, high DFF yield

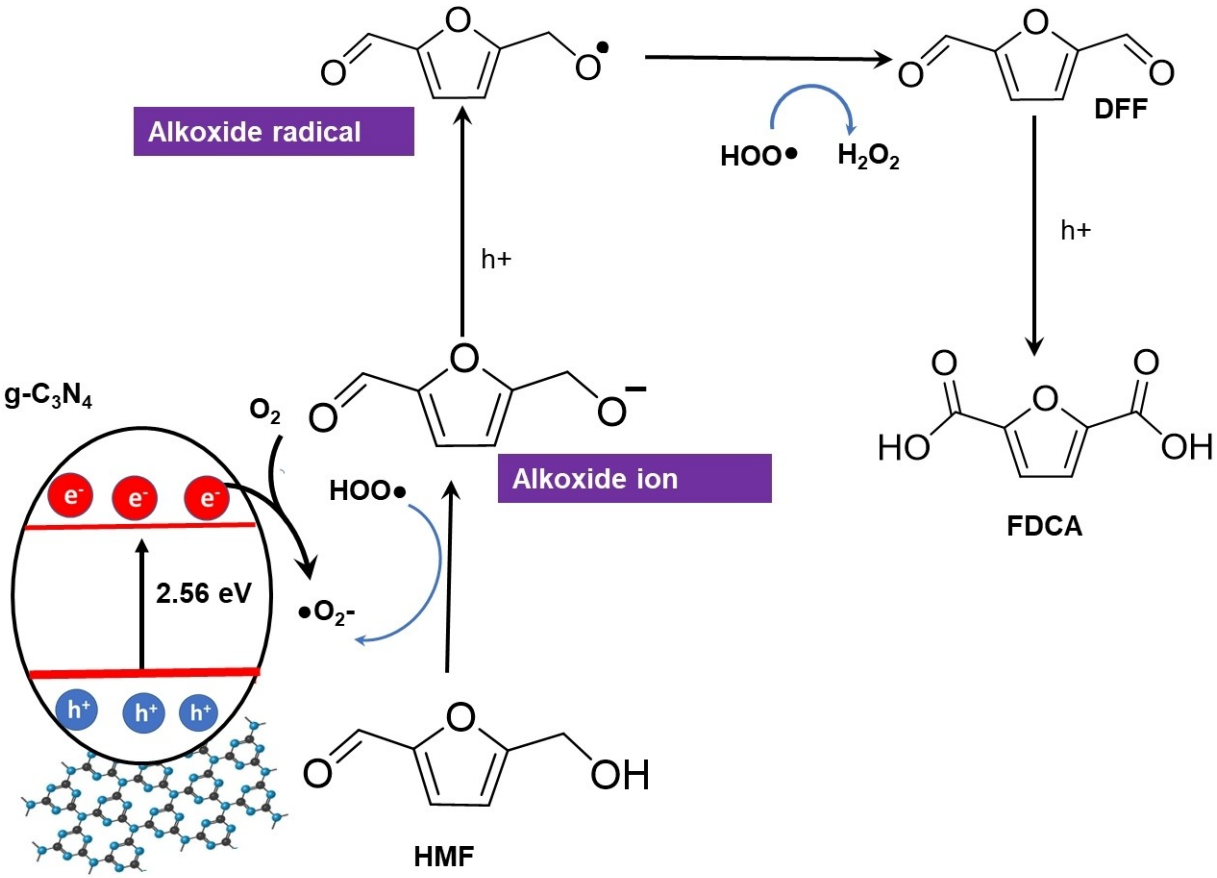

Scheme 4. Photocatalytic selective oxidation of HMF-DFF/FDCA over g-C_3N_4 photocatalyst.[90] Adapted with permission from Molecular Catalysis.

was recorded via the cooperative interplay between alkoxide intermediates and controlled $^{\bullet}O_2^-$ production. However, under UV light conditions, high overoxidation of DFF to FDCA was observed. The unique 2D structure of g-C_3N_4, visible light responsiveness and moderate band gap, enable the reduction of O_2 to $^{\bullet}O_2^-$ at the CB. As depicted in Scheme 4, HMF was first deprotonated by a photogenerated hole (h^+) to a proton (H^+) forming an alkoxide anion, and the formed alkoxide anion reacts with the h^+ to form the alkoxide radical intermediate. The alkoxide radical further recombines with superoxide radicals, resulting in the production of DFF which is subsequently converted to FDCA by the generated H_2O_2.

The plasmonic surface resonance photocatalytic design has been explored in tandem to promote the conversion of carbohydrates to sugars and also furanic derivatives in some recent studies. Zhou et al.[86] observed high selectivities via the simultaneous conversion of glucose, 2-furaldehyde, xylose, HMF, and furfural alcohol to their corresponding carboxyls using Au/TiO_2 as photocatalyst and Na_2CO_3 as an additive. Higher selectivity (>95 %) was observed under both visible light and UV irradiations, with Na_2CO_3 playing a significant role in inhibiting highly oxidative ROSs. Consequently, the coupled migration of electrons into the conduction band of TiO_2 and the plasmonic surface resonance of Au-nano particles enhanced UV light and visible light responsiveness, respectively. Mechanistic studies further showed that oxygen radical production led to the cleavage of bonds in the various substrates.

2.3.3. Photo-conversion of biomass to fuel (hydrogen gas)

Photo-splitting of H_2O results in low yields of hydrogen gas and has not been performed extensively on an industrial scale due to the use of expensive noble metals (Pt, Ir, Pd, Ru, etc), slow kinetics, and the need for hole scavengers.[104,105] Biomass such as sugars, lignocellulose and alcohols have been incorporated to scavenge or consume holes to pave the way for electrons to reduce protons to H_2. Comprehensive reviews on photocatalytic biomass conversion to H_2 as an alternative to fossil fuels have been reported elsewhere.[106,107] Comparatively, polysaccharide-based biomass conversion to H_2 dominates the use of lignin. For instance, an obtained acid hydrolysate from pine wood (containing xylose and glucose) was adopted and used in a photocatalytic process with TiO_2, affording 19.9 mL of H_2/g of pine wood substrate. The glucose and xylose served as hole scavengers, thereby enhancing performance.

Iervolino[84] performed a reaction under visible and UV radiation conditions where glucose was successfully photo-converted into H_2 over a Ru-doped $LaFeO_3$ catalyst,

producing higher yields than $LaFeO_3$ alone. Overall, the yield of hydrogen reached 910 $\mu mol\,h^{-1}\,g_{cat}^{-1}$. Mechanistically, the production of Ru^{3+} available in the $LaFeO_3$ crystalline structure acted as an electron scavenger, which was able to limit the recombination of electrons and holes. Recently, novel non-noble photocatalytic systems have been reported for the concomitant evolution of hydrogen and value-added chemicals. P-doped $Zn_xCd_{1-x}S$ with sulfur-rich vacancies was demonstrated to facilitate the conversion of HMF to DFF and H_2O splitting which fulfills the dual strategy without the addition of any external electron donor.[87] A high yield of H_2 (419 $\mu mol\,h^{-1}\,g^{-1}$) was achieved using $Zn_{0.5}Cd_{0.5}S$–P as a photocatalyst, and the addition of HMF into the catalytic system significantly enhanced yield to 786 $\mu mol\,h^{-1}\,g^{-1}$, alongside the production of DFF. Aside from this, glucose has been used to produce hydrogen as highlighted in Table 3. Hao et al.[79] via chemisorption of sulfate (SO_4^{2-}) and nickel sulfide (Ni_xS_y) modified TiO_2 (thus Ni–S/TiO_2) and used it for cellulose photo-reforming to hydrogen. An impressive yield of H_2 (3020 $\mu mol\,h^{-1}\,g_{cat}^{-1}$) was achieved and this was 76 times higher than using TiO_2 alone. The SO_4^{2-} provided the acid site for hydrolyzing cellulose to glucose and further accessibility of substrate by photocatalyst, while the Ni_xS_y helped to trap electrons and also played the role of a co-catalyst for H_2 production. Incorporating a layer of a graphitic carbon onto NiO_x/TiO_2 was reported to facilitate the weakening of O–H in saccharides and alcohols, with high H_2 evolution of 270 and 4150 $\mu mol\,h^{-1}\,g_{cat}^{-1}$. at room temperature and 80 °C temperature, respectively. As shown in Scheme 5a, the dehydrogenation reaction via the abstraction of a proton and formation of alkoxide anions reduces Ni sites producing Ni–H and affording a high yield of H_2.[80] Also, Zhang et al.[104] observed a similar mechanistic pathway using a g-C_3N_4 modified with non-noble metal (Ni/g-C_3N_4) noble metal (Ni/g-C_3N_4) photocatalyst to convert HMF to DFF (Scheme 5b). The HMF was first activated by a photogenerated hole (h^+) to a proton (H^+) and alkoxide radical intermediate, and the formed alkoxide radical intermediate can further be oxidized to DFF by superoxide radicals, indicating the tandem roles of ROSs, and this intermediates. Meanwhile, other products such as CH_4, CO_2, and CO were formed by the photogenerated holes.

Regarding the photo-conversion of lignin to H_2, a combination of different valuable products (H_2, CH_4, and fatty acids) have been reported from a photo-reforming experiment applying TiO_2@NiO heterojunction as photocatalyst and Kraft lignin as feedstock.[108] The synthesized TiO_2@NiO heterojunction facilitated effective redox reactions via electron-hole separation and migration, while the

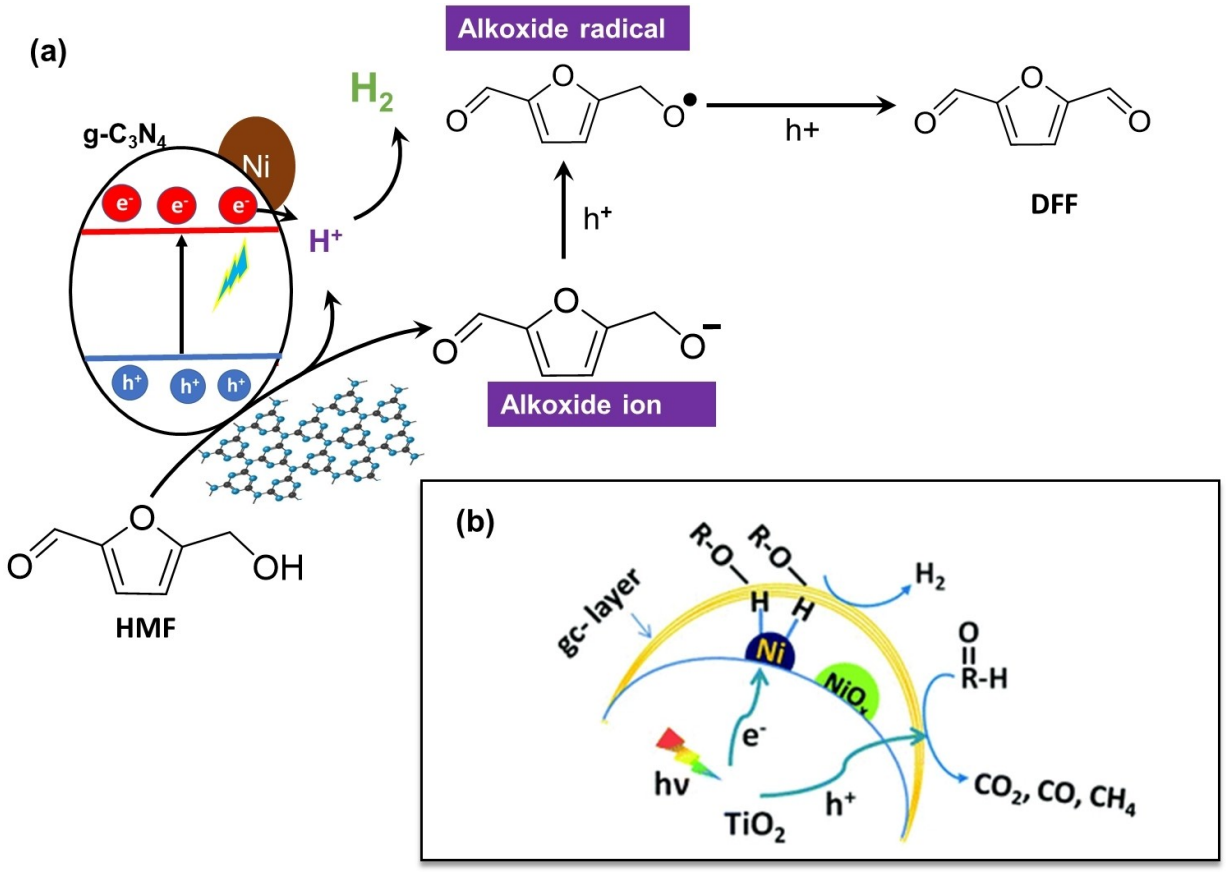

Scheme 5. Concomitant photocatalytic evolution of H_2 and value-added chemicals in the absence of noble precious metals. a) Dehydrogenation of HMF to DFF over Ni/g-C_3N_4.[104] b) $TiO_2/NiO_x@C_g$ photocatalytic promoted the evolution of H_2 from cellulose.[80] Adapted with permission from the Royal Society of Chemistry (Greem Chemistry, 2018 and 2021).

formation of H_2 is stimulated by the formation of electrons on the surface of TiO_2. However, it has been reported that photocatalytic conversion of lignin works effectively using metallic sulfides as photocatalysts. Li et al.[109] reported that the activity of NiS (20 % loading)/CdS is 5041 times higher with apparent quantum efficiency (AQE) of 44.9 % than pristine CdS on the conversion of lignin to H_2. A major drawback with the use of sulfide-based photocatalysts (e.g. CdS, which is undoubtedly the most applied metal sulfide for biomass conversion) is the onset of photo-corrosion, which needs greater attention. Wakerley and colleagues[110] reported a successful conversion of native lignocellulosic biomass which was photo-reformed using CdS/CdOx QDs (260 $\mu mol\,h^{-1}\,g_{cat}^{-1}$) and showed higher performance than $TiO_2\,|\,RuO_2$–Pt catalyst. In situ formation of CdO_x on the surface of CdS QDs was observed when pH was increased to 14 (Figure 6). Consequently, the formation of CdO_x on the surface led to resistance in photo-corrosion together with the enhanced formation of H_2, and this could be a promising route to overcoming photo-corrosion in metal sulfides. Since most lignin remains insoluble in aqueous solvents, working at elevated pH could also enhance the dissolution of lignin to create adequate contact between the catalyst and lignin.

3. SWOT Analysis of the Photocatalytic Process

To translate the gained scientific findings into a competitive large-scale application, a suitable SWOT (strength, weaknesses, opportunities, and threats) analysis with an emphasis on its application for biomass conversion would be highly beneficial.[111,112] Figure 7a summarises the SWOT analysis for evaluating the feasibility of photocatalytic biomass conversion technology. Photocatalytic biomass conversion to value-added chemicals was benchmarked with thermochemical strategies, while for discussions involving the concomitant conversion of biomass to value-added chemicals and hydrogen, we benchmarked both thermochemical and conventional water splitting systems. In the following points, strengths, weaknesses, opportunities and threats are critically discussed to facilitate the comparison with existing technologies and the transfer of this technology to a large scale.

3.1. Strengths

Biomass conversion by heterogeneous photocatalysis shows some pros as compared to conventional thermocatalytic processes. Based on this SWOT assessment, the strength of photocatalytic technology toward biomass conversion could be summarized as follows:

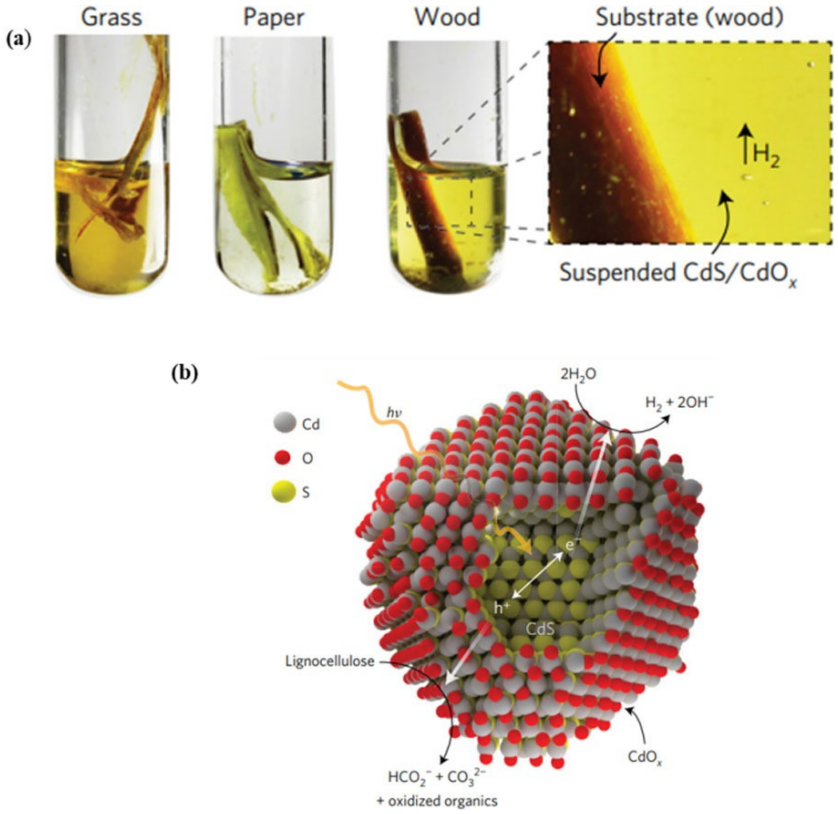

Figure 6. Solar-light photocatalytic conversion of native biomass to H_2 over CdS/CdO_x.[110] a) The robust catalytic system enhanced H_2 evolution from different native biomass substrates under basic conditions. b) Mechanism showing CdS/CdO_x with –OH functionalities available on the surface of CdO_x. Adapted with permission from Springer Nature.

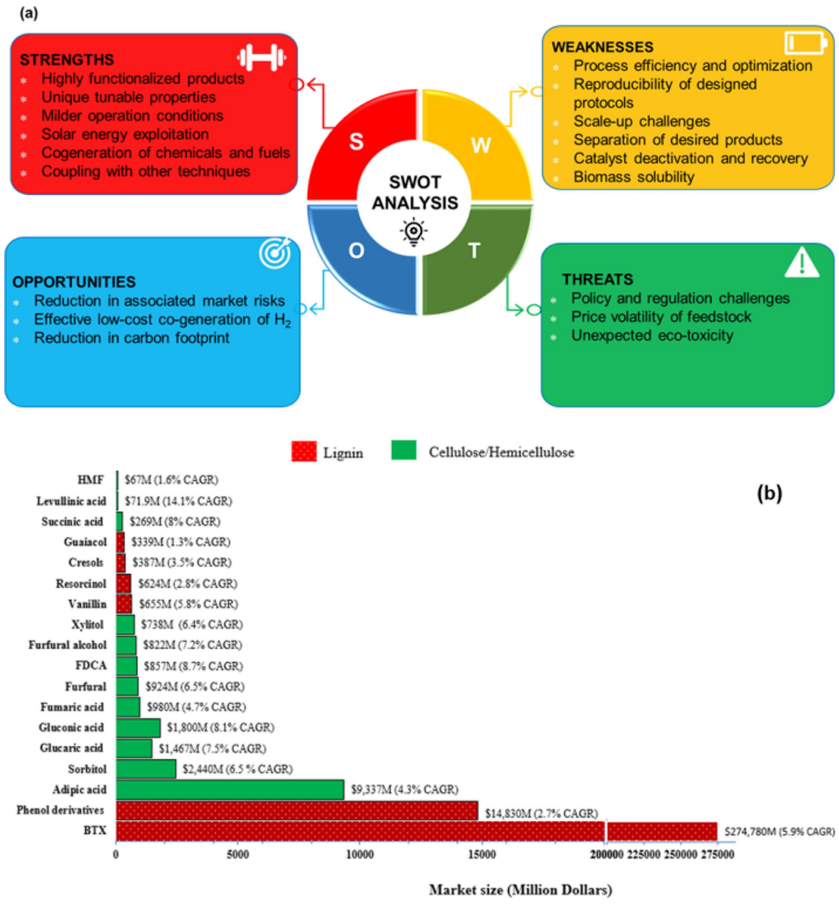

Figure 7. Commercial scale feasibility of photocatalysis biomass conversion and market growth of biomass-derived chemicals. a) SWOT (Strengths-Weaknesses-Opportunities-Threats) matrice built for photocatalysis as a biomass conversion technology. b) Market size and compound annual growth rate (CAGR%) of highly promising photocatalysis value-added chemicals (2018–2028). BTX,[113] Phenol derivatives,[114] Adipic acid,[115] Sorbitol,[116] Glucaric acid,[117] Gluconic acid,[118] Fumaric acid,[119] Furfural,[120] FDCA,[121] Furfural alcohol,[122] Xylitol,[123] Vanillin,[124] Resorcinol,[125] Cresols,[126] Guaiacol,[127] Succinic acid,[128] Levullinic acid,[129] HMF.[130]

- **Highly functionalized products**: Photocatalysis can exclusively promote the cleavage of specific bonds of biomass which leads to producing highly functionalized high-value products. Based on the conducted summaries provided, while photocatalytic conversion of lignin typically produces aromatic aldehydes and aromatic ketones, other report shows that using robust conditions such as thermochemical processes results in products such as benzene, toluene, and xylene which require further functionalization,[131] thereby making the process costly.
- **Unique tunable properties**: The unique ability to control the type or/and number of ROSs and radical intermediate formation is plausible through the design of materials with required characteristics, i.e., modification of photocatalyst surfaces, band gap engineering and playing on the heterojunction systems such as the ratio, level of CB/VB and so on.
- **Milder operation conditions**: Due to the abundance of robust C–C bonds, a high number of oxygen-containing functional groups, and the complexity of biomass, the scission of bonds in most biomass reactions require a temperature of more than 160 °C and high chemical consumption; however, these reactions can take place at room temperature via photocatalysis. Unlike other processes, photocatalysis does not require high energy consumption as it works at mild conditions, nor the excessive usage of organic solvent. On top of this, appropriate design of photocatalysts and reaction conditions could be used to control radical formation and selectivity, a characteristic that is not common in thermocatalytic systems.
- **Cogeneration of chemicals and fuels**: Due to the redox system of photocatalysis, the co-generation of many high-value products could take place simultaneously, and the concept of full valorization of biomass could be obtained under some optimized circumstances, i.e., co-generation of phenolic compounds via ROSs mediated reaction and H_2 via band gap reductive reaction and evolution of specific ROSs. For instance, in the case of HMF dehydrogenation reactions, superoxide radicals and the formation of alkoxide radicals using g-C_3N_4 play a significant role. Based on numerous critical reports, direct H_2 evaluation from water suffers from low production yields, unless the reaction is balanced by the addition of

large quantities of hole scavenger molecules with strong affinities as ROSs/hole scavengers to liberate and avoid the quick recombination of e−/h+. In addition, the set-up and installations of large-scale reactors and the required conditions would not be economical. Recently, Bie and colleagues[132] subtly provided a critical review on this subject arguing why water splitting via photocatalysis is practically and theoretically hard to achieve on large-scale. The slow kinetics, rapid back reactions, unfavorable thermodynamics, and dissolved oxygen, remain the major challenges supporting this argument. By contrast, the concomitant conversion of biomass to value-added chemicals and H_2 represents an emerging technology with most work undertaken on a milligram-gram scale. Meanwhile, the cogeneration reaction can proceed via a single electron which is an easier option than four-electron oxygen evolution.

– **Flexible coupling strategy**: The flexibility of photocatalysis allows it to be incorporated or combined with different processes. Hence, it could be combined with other emerging or existing technologies to enhance conversion efficiency, promote the complete conversion of biomass, expand the product range, and increase the economic viability of the process. Several successful combinations have been reported with outstanding advantages such as sono-photocatalysis, photoelectrochemical, photothermal-photocatalysis, and so on. In conventional biorefineries, this technology has been reported to enhance ethanol yield from biomass. Yasuda et al.[133] applied TiO_2-based photocatalysis for pretreating silver and Napier grass and this was reported to enhance enzymatic hydrolysis and subsequent fermentation.[133] Shiamala et al.[134] also reported enhanced ethanol fermentation and anaerobic digestion via the conversion of starch to smaller molecules in the presence of TiO_2/Bi_2WO_6 under visible light conditions. The promotional effect of combining photocatalysis with electrocatalysis for biomass depolymerization has been extensively reviewed.[135] Sono-photocatalytic pretreatment to enhance the conversion of biomass in terms of yield and fast kinetics was recently critically discussed in our review.[136] The use of sono-photocatalysis is reported to reduce photocatalyst deactivation via enhanced generation of ROSs.[137] In addition, coupling mechanocatalysis with photocatalysis to enhance the yield of high-value platform chemicals could lead to synergetic and enhanced conversion as reported in our recent study.[138]
– **Solar energy exploitation**: Finally, the use of inexhaustible solar light to catalyze biomass conversion is considered a green and cheap technology that supports sustainable development. The potential utilization of solar light could make the process an energy-saving and highly sustainable process as compared to other robust conventional processes. As discussed above, the direct use of sunlight for biomass conversion has been presented and explored for value-added chemicals, H_2 production, and concomitant production of hydrogen and value-added chemicals.[110] This makes photocatalysis an intriguing technology for the energy sector if it gradually emerges as a commercial technology for biomass valorization to fuels and platform chemicals.

3.2. Weaknesses

Photocatalytic biomass conversion has the potential to be a sustainable and efficient process however, some significant challenges to make this technology cost-effective and more practical remain. The key weaknesses of photocatalytic biomass conversion could be described as follows:

– **Process efficiency and optimization challenges**: The quality and yield of desired products against the used native biomass would be also a serious issue limiting the commercial viability of the photocatalysis process. One of the weaknesses of photocatalytic technology towards the conversion of native biomass is the non-uniformity of the reaction because of the uncontrolled factors in terms of the type of biomass or variation of irradiation intensity if direct solar light is used. The optimization and the control of the photocatalytic system are still challenging up to date, especially if native biomass is targeted. As discussed, most of the prevailing studies on photocatalysis have been done using model compounds instead of raw/native biomass. This is due to the complexity of native biomass, impurities such as sulfur, nitrogen, and metal ions may persist in it, and this is likely to scavenge the formation and action of ROSs during photocatalysis.[17,139] The solid suspension can limit the penetration of light irradiation to the surface of the photocatalyst, and also ROSs attack on biomass polymer would be weaker as compared to lab-scale small reactors. As an important step for biomass conversion, the optimization of photocatalysis requires careful optimization of key operating conditions such as temperature, the intensity of light irradiation, and catalyst loading, which can be costly and energy-consuming. Photocatalysis requires efficient light irradiation, however, products, solvents, materials, and photosensitizers could all act as filters, which can become pronounced on large-scale.
– **Challenges in reproducing photocatalytic protocols**: Compared to most conventional processes such as thermo-promoted reactions, photocatalytic protocols/methods could be difficult to replicate by other groups. This challenge erupts due to the high dependence of catalytic reactions on the experimental set-up and catalytic design. An ideal solution to this challenge could be the design of a standardized reactor for unique reactions however, this has not been possible due to the low-cost making reactors by most researchers. Aside from reactors, there exists no unified standard for selecting lights such as LEDs used to have different specifications, as pointed out by Reischauer et al.[20]
– **Scale-up challenges and design of photocatalytic devices**: Unlike other conventional approaches, the scale-up demonstration of photocatalysis conversion of biomass at pilot and commercial levels is rare. Overall, translating findings from laboratory scale to commercial status remains a daunting task. More to this, the identification

of a more reliable method to realize the rational design of a photocatalyst for biomass conversion remains a key obstacle. Researchers have focused on the development of different photocatalytic materials to identify their surface properties and associated mechanisms. However, none of these catalysts have yet been selected for industrial applications due to their complicated preparations, low efficiency, low stability, etc. Large-scale synthesis of catalysts using commonly used methods such as hydrothermal and other combustion techniques is not ready for large-scale production.[140] Moreover, large-scale photocatalytic biomass conversion requires the use of high-intensity light and long reaction time, which may reduce the efficiency of the entire process as discussed before. It is worthy to mention that not the same products can be obtained if the biomass origin is different. The cost of the process against the income in terms of produced high-value products would be a serious threat even though the photocatalytic systems seem non-costly, but at large-scale further complications could be faced. For example, the design of innovative large-scale reactors for this purpose needs serious consideration to ensure high efficiency and production uniformity.

- **Separation of desired products**: The difficulty in controlling radical intermediates and unwanted side reactions leads to produce a huge number of wanted and unwanted compounds which are obtained in the final mixture. It is worth mentioning that the separation of these compounds is a very complicated and costly process.
- **Catalyst deactivation and recovery**: Like all heterogeneous catalytic-based processes, in biomass conversion, the yield and the quality of products could be reduced within the irradiation time because of the degradation or inactivation of the catalyst surface. Many studies report effective and selective photocatalytic-based materials, but they can't be considered at a large scale because of several factors including the cost, the less availability, the low stability, complicated synthesis, and so on. Catalyst deactivation could be triggered by surface corrosion or adsorption of substrates and formed products onto the surface of the catalyst. Additionally, metallic sulfide-based photocatalysts (e.g. CdS) are reported to suffer from frequent photo-corrosion caused by photogenerated holes[45] If the adsorption of products on the surface of the photocatalyst increases and become resistant to photo-produced ROSs, deactivation could be more pronounced.[141] The use of photoredox catalysts with tunable properties (such as Ir-based metal complexes, Ru-based complexes, etc) for controlling intermediate formation in biomass conversion is gaining significant interest as discussed above. Additionally, the design of most catalytic systems for H_2 evolution relies on the incorporation of highly costly and non-scalable noble precious metals (Pt, RuO, Pd).[142,143] Based in European recommendations, some of these metals are regarded as critical metals for short and long-term sustainable biomass-based chemical and fuel transitioning.[144] An alternative could have been intensifying the strategies for recovering this photocatalyst, however little attention has been paid to the developing recovery of photocatalysts during biomass conversion. Even though heterogeneous catalysts have the advantage to be recovered, at a large scale, it is very hard to recover nano-sized particles, i.e., TiO_2, which needs a costly membrane filtration.
- **Biomass solubility and high use of organic solvents/chemicals**: The dissolution of biomass in water is very challenging even at the lab scale; therefore, the use of some organic solvents is required which in turn might lead to affect the ROSs attack process due to the scavenging effects, and it might produce new unwanted byproducts in the medium. The sustainability of the process would be different at a large scale wherein huge volumes of organic solvents are used to dissolve biomass blocks which in turn can affect the ROSs role in biomass bonds cleavage.[80] Meanwhile, the identification of a mild and efficient method for solubilizing biomass without destroying β-O-4 bonds in the case of lignin depolymerization is becoming a strong hindrance before photocatalytic reaction.[59]

3.3. Opportunities

Opportunities reflect favorable external factors which could give the photocatalytic technology a competitive advantage in the future over conventional processes. Tentatively, the adoption of photocatalysis as a biomass conversion technology can contribute significantly to sustainable development and transitioning to low carbon economy via the many opportunities discussed below:

- **Reduction in associated market risks**: The main opportunity to scale up the photocatalytic technology towards biomass valorization is the design of systems that can produce effectively different desired products under multi scenarios and conditions. This technology can provide investors or consumers the chance to withstand the shock of rapidly changing or emerging market trends for value-added chemicals and fuels. Based on reviewed data, Figure 7b depicts the forecasted global market values for key commercially feasible chemicals obtained from biomass valorization and their compound annual growth rate (CAGR %) between the years 2018–2028. Biomass conversion can provide a wide range of products. It is important to stress that photocatalytic technology can produce most of the products which could not be obtained through biomass conversion using other existing and emerging technologies. In this sense, photocatalysis could be a feasible option to withstand market shocks.
- **Effective low-cost co-generation of H_2**: Based on numerous critical reports, direct H_2 evaluation from water suffers from the low production yield, unless the reaction is balanced by the addition of large quantities of hole scavenger molecules with strong affinities as ROSs/hole scavengers to liberate and avoid the quick recombination of e-/h+. In addition, the set-up and installation of large-scale reactors and the required conditions would not be economical. In a biomass conversion system, the abundant biomass derivatives can catalyze the production of

H_2 without the need the use sacrificial reagents. The incorporation of sacrificial agents may enhance yield but result in uncontrollable environmental pollution.[145–147] Therefore, under appropriate circumstances, H_2 can be co-produced during the conversion of biomass into desired products. As an industrial opportunity, the co-generation of H_2, as an integrated system, during the photocatalytic conversion of biomass wastes into valuable products could be more economically interesting as compared to single photocatalytic H_2 evaluation from direct water splitting.

- **Reduction in carbon footprint**: From a green chemistry perspective, photocatalytic biomass conversion can contribute significantly by reducing the high use of toxic chemicals or harsh reaction conditions (pressure and temperature) which pose a significant threat to the environment, as opposed to conventionally used thermochemical/thermocatalytic processes. Aside from the unique ability to reduce the high dependence on chemicals or high pressure during the conversion of biomass, the option to concomitantly produce value-added chemicals and hydrogen can reduce the carbon footprint of the chemical industry which currently relies on fossil-based sources, alongside the reduction of greenhouse emission. As a clean and carbon-free option, green hydrogen from hydrogen will play an important role in the energy demand for humankind. Meanwhile, when combined with other technologies likely, photocatalytic biomass conversion can even go higher to reduce greenhouse gas emissions. Photocatalytic technology can promote a circular bioeconomy since it could promote the depolymerization of biomass, upgrade platform building blocks, and recycle polymers back to their respective monomers, ensuring the reusability of monomers.[148,149] This will help in the development of a sustainable circular bioeconomy where there is no waste production via recycling and reuse.

3.4. Threats

While photocatalysis has shown several opportunities for biomass conversion, numerous and significant potential threats pertain to the future adoption of this on a large scale. As above mentioned in sub-sections, at a large scale, we may expect several threats at different process stages as summarized in the following points:

- **Policy and regulation challenges**: Although photocatalytic biomass conversion looks promising, the regulations for the adoption of this technology on a large scale may still be evolving, which in general creates a lot of uncertainties regarding the requirements for the adoption of this technology. This threat could hinder entry and also limit investments in adopting this technology.
- **Competition from other mature technologies**: Unlike some conventional processes, photocatalysis might require some time to be able to attain market readiness and acceptance. Also, we project that competition with other existing technologies such as thermochemical/thermocatalytic process as it is already known at large scale.
- **Price volatility of feedstock**: Since most biomass conversion technologies are still maturing, feedstock prices may likely be volatile in the future which can impact the economic viability and the adoption of large-scale projects.
- **Unexpected eco-toxicity**: Even though photocatalysis stands a greater advantage over conventional thermocatalytic strategies, some photocatalytic-based materials (such as solvents, metals and and nano-size materials) can be harmful to humans or the environment in general if not handled/disposed of carefully. Numerous diversities of photocatalysts have been reported for biomass conversion to value-added chemicals and fuels, and accompanying this could be growing concerns of potential toxicity to humans and the environment at large. Some recent reviews on the ecotoxicity of photocatalysts have been reported.[145–147] Soluble nanoparticles are more toxic in the cellular environment than insoluble nanoparticles. Such unexpected toxicity may be erupting and this could impede the future adoption of highly-performing photocatalysts.

4. Conclusions and Perspectives

Novel strategies leading to the development of environmentally friendly and economically viable biomass photocatalytic conversion techniques have been critically analyzed. Through the unified approach of utilizing photocatalysis for biomass conversion conducted in this review, we identified key scientific challenges which have been tackled relatively well, and those needing attention for further application of photocatalysis in industrial settings and smooth transitioning to circular bioeconomy sustainably. Photocatalysis has shown an attractive pathway for transforming different fractions of biomass. Photo-induced ROSs and other substrate-based radical intermediates have been important in promoting the selective oxidation of biomass. Mechanisms such as proton-coupled electron transfer (PCET), ligand-to-metal charge-transfer (LMCT), single-electron transfer(SET), and π–π stacking have been key in controlling the formation of alkoxy radical intermediates leading to the cleavage of C_α–C_β and C–O interlinkages in β-O-4 and β-1 model lignin. Photocatalytic plasmonic thermal effect generation looks promising for one-pot conversion of polysaccharides, especially overcoming the challenges associated with the conversion of biomass to furan derivatives, which have so far been achieved via three separate steps (pretreatment, hydrolysis into sugar, and conversion of sugars into chemicals). The use of noble metals and metal oxides has an established foundation, however, the emerging role of g-C_3N_4 looks promising for the co-generation of H_2 and platform chemicals in addition to its economic advantage. The unique cooperative interplay of superoxide radicals and the formation of alkoxide radicals promote the partial oxidation of furanic compounds. Meanwhile, the two-fold strategy for photo-conversion of biomass and water splitting

to value-added chemicals and hydrogen looks more promising than water splitting alone systems.

Despite the progress made by the scientific community to develop photocatalysis as a biomass valorization technique, some critical weaknesses which need further research are comprehensively presented in Figure 8. Importantly, to enhance the efficiency of photocatalytic valorization of LCB, the use microfluidic reactor design is recommended.[150,151] As reported, this type of reactor provides enhanced mass and heat transfer between photocatalyst and LCB, and this can boost the photocatalytic performance. Also, the development of strategies for in situ collection, storage, and utilization of H_2 needs more attention from the scientific community as we target large-scale production, profitability, and safety of the whole process. On top of that, other combined issues such as the development of multifunctional catalysts, reactor engineering, feedstock purification, and recycling of photocatalysts, type of reaction, geometry, and way of use need to be taken into consideration, along with the optimization of factors of the photocatalytic process including all details such as speed of stirring, the quantity of photocatalyst, type of irradiation and distance, the quantity of biomass to be treated per time and so on.

Further research into the development of mild coupling techniques may be needed to enhance solubility, purify biomass against radical scavengers, and enhance biomass pre-oxidation. Moreover, studies into coupling systems such as photo-electrocatalysis, sono-photocatalysis, photo-biocatalysis, and others are encouraged. Meanwhile, expanded research on the identification of a simple technique for purifying and separating platform chemicals from a reaction media after photocatalytic conversion of LCB is needed. Regarding ROS formation and control, more work may be needed to extensively control the formation and action of these radicals, especially for one-pot or in situ oxidation of C_β–O and C_α–C_β bonds in biomass. Additionally, attention should be paid to developing non-noble plasmonic photocatalysts for biomass conversion. The scientific community is required to work closely with industries to understand any raised issues and also to remain in touch with novel industrial concepts and sustainable development. Opportunities could be developed and widened through large experience, rather than over experimentation at a lab scale. In addition, for industrial-scale applications, the scalability and economic feasibility of photocatalytic biomass conversion should be expanded using other sophisticated strategies (life-cycle- and techno-economic analyses) because data on this aspect is rare in most photocatalytic biomass conversion studies. We anticipate that the different strategies for enhancing photocatalytic oxidation via selective bond cleavage reported here will rekindle significant industrial interest in exploring selective oxidation and associated strategies for the profitable application of photocatalysis as a commercial technology for LCB.

Acknowledgements

Dominic Aboagye is grateful for the support from Universitat Rovira i Virgili Marti Franques Grant No. 2019 PMF-PIPF-15. Appreciations to Grant PID2021-123665OB-I00 funded by MCIN/AEI/ 10.13039/501100011033 and by "ERDF A way of making Europe" and Diputació de

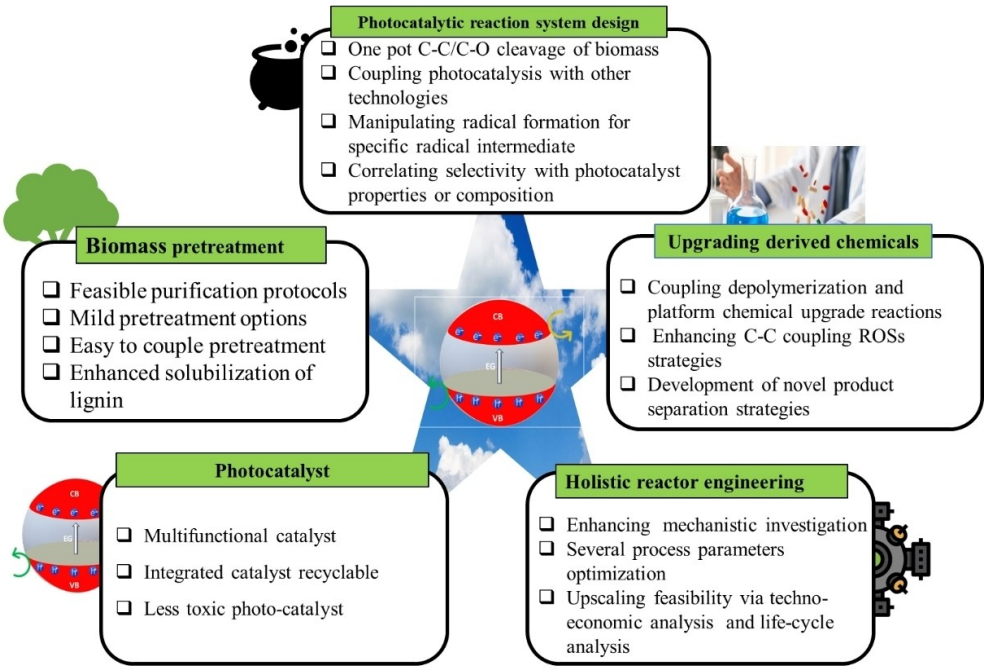

Figure 8. Our comprehensive approach to developing photocatalysis for full lignocellulose biomass conversion into different platform chemicals and fuels.

Tarragona with reference 2021/03 for funding this research. Dr Ridha Djellabi acknowledges Maria Zambrano Grants-2021URV-MZ-15.

Conflict of Interest

The authors declare no competing interests.

Data Availability Statement

Data sharing is not applicable to this article as no new data were created or analyzed in this study.

Keywords: Hydrogen · Lignocellulose · Photocatalysis · Radical Oxygen Species · Value-Added Chemicals

[1] J. Sherwood, *Bioresour. Technol.* **2020**, *300*, 122755.
[2] D. D'Amato, N. Droste, B. Allen, M. Kettunen, K. Lähtinen, J. Korhonen, P. Leskinen, B. D. Matthies, A. Toppinen, *J. Cleaner Prod.* **2017**, *168*, 716–734.
[3] N. Dahmen, I. Lewandowski, S. Zibek, A. Weidtmann, *GCB Bioenergy* **2019**, *11*, 107–117.
[4] L. A. Zevallos Torres, A. Lorenci Woiciechowski, V. O. de Andrade Tanobe, S. G. Karp, L. C. Guimarães Lorenci, C. Faulds, C. R. Soccol, *J. Cleaner Prod.* **2020**, *263*, 121499.
[5] L. Bhatia, V. K. Garlapati, A. K. Chandel in *Horizons in Bioprocess Engineering* (Ed.: R. Pogaku), Springer, Cham, **2019**, pp. 73–90.
[6] P. Gallezot, *Chem. Soc. Rev.* **2012**, *41*, 1538–1558.
[7] C. O. Tuck, E. Pérez, I. T. Horváth, R. A. Sheldon, M. Poliakoff, *Science* **2012**, *337*, 695–699.
[8] C. Liu, S. Wu, H. Zhang, R. Xiao, *Fuel Process. Technol.* **2019**, *191*, 181–201.
[9] J. J. Bozell, G. R. Petersen, *Green Chem.* **2010**, *12*, 539–554.
[10] M. I. Alam, S. De, T. S. Khan, M. A. Haider, B. Saha, *Ind. Crops Prod.* **2018**, *123*, 629–637.
[11] C. Chen, L. Wang, B. Zhu, Z. Zhou, S. I. El-Hout, J. Yang, J. Zhang, *J. Energy Chem.* **2021**, *54*, 528–554.
[12] M. V. Galkin, J. S. M. Samec, *ChemSusChem* **2016**, *9*, 1544–1558.
[13] S. Gazi, *Appl. Catal. B* **2019**, *257*, 117936.
[14] C. F. Shih, T. Zhang, J. Li, C. Bai, *Joule* **2018**, *2*, 1925–1949.
[15] N. P. Brandon, Z. Kurban, *Philos. Trans. R. Soc. London Ser. A* **2017**, *375*, 20160400.
[16] I. Staffell, D. Scamman, A. V. Abad, P. Balcombe, P. E. Dodds, P. Ekins, N. Shah, K. R. Ward, *Energy Environ. Sci.* **2019**, *12*, 463–491.
[17] L. I. Granone, F. Sieland, N. Zheng, R. Dillert, D. W. Bahnemann, *Green Chem.* **2018**, *20*, 1169–1192.
[18] J. R. Banu, S. Kavitha, R. Y. Kannah, T. P. Devi, M. Gunasekaran, S. H. Kim, G. Kumar, *Bioresour. Technol.* **2019**, *290*, 121790.
[19] D. Aboagye, F. Medina, S. Contreras, *Catal. Today* **2022**, *413–415*, 113969.
[20] S. Reischauer, B. Pieber, *iScience* **2021**, *24*, 102209.
[21] G. C. de Assis, I. M. A. Silva, T. G. dos Santos, T. V. dos Santos, M. R. Meneghetti, S. M. P. Meneghetti, *Catal. Sci. Technol.* **2021**, *11*, 2354–2360.
[22] A. L. Barthelemy, B. Tuccio, E. Magnier, G. Dagousset, *Angew. Chem. Int. Ed.* **2018**, *57*, 13790–13794.
[23] H. Yi, G. Zhang, H. Wang, Z. Huang, J. Wang, A. K. Singh, A. Lei, *Chem. Rev.* **2017**, *117*, 9016–9085.
[24] Z. Huang, Y. Yang, J. Mu, G. Li, J. Han, P. Ren, J. Zhang, N. Luo, K. L. Han, F. Wang, *Chin. J. Catal.* **2023**, *45*, 120–131.
[25] S. Li, Z. J. Li, H. Yu, M. R. Sytu, Y. Wang, D. Beeri, W. Zheng, B. D. Sherman, C. G. Yoo, G. Leem, *ACS Energy Lett.* **2020**, *5*, 777–784.
[26] M. F. Kuehnel, E. Reisner, *Angew. Chem. Int. Ed.* **2018**, *57*, 3290–3296.
[27] S. Clair, D. G. De Oteyza, *Chem. Rev.* **2019**, *119*, 4717–4776.
[28] M. H. Shaw, J. Twilton, D. W. C. MacMillan, *J. Org. Chem.* **2016**, *81*, 6898–6926.
[29] L. J. Rono, H. G. Yayla, D. Y. Wang, M. F. Armstrong, R. R. Knowles, *J. Am. Chem. Soc.* **2013**, *135*, 17735–17738.
[30] Z. Huang, N. Luo, C. Zhang, F. Wang, *Nat. Rev. Chem.* **2022**, *6*, 197–214.
[31] B. Ohtani, *Phys. Chem. Chem. Phys.* **2014**, *16*, 1788–1797.
[32] M. Mazarji, M. Alvarado-Morales, P. Tsapekos, G. Nabi-Bidhendi, N. M. Mahmoodi, I. Angelidaki, *Environ. Int.* **2019**, *125*, 172–183.
[33] F. Collin, *Int. J. Mol. Sci.* **2019**, *20*, 2407.
[34] M. Yan, J. C. Lo, J. T. Edwards, P. S. Baran, *J. Am. Chem. Soc.* **2016**, *39*, 12692–12714.
[35] V. K. Ponnusamy, D. D. Nguyen, J. Dharmaraja, S. Shobana, J. R. Banu, R. G. Saratale, S. W. Chang, G. Kumar, *Bioresour. Technol.* **2019**, *271*, 12692–12714.
[36] S. Liu, L. Bai, A. P. van Muyden, Z. Huang, X. Cui, Z. Fei, X. Li, X. Hu, P. J. Dyson, *Green Chem.* **2019**, *21*, 1974–1981.
[37] R. Rinaldi, R. Jastrzebski, M. T. Clough, J. Ralph, M. Kennema, P. C. A. Bruijnincx, B. M. Weckhuysen, *Angew. Chem. Int. Ed.* **2016**, *55*, 8164–8215.
[38] R. Asahi, T. Morikawa, T. Ohwaki, K. Aoki, Y. Taga, *Science* **2001**, *293*, 269.
[39] M. Ksibi, S. ben Amor, S. Cherif, E. Elaloui, A. Houas, M. Elaloui, *J. Photochem. Photobiol. A* **2003**, *154*, 211–218.
[40] J. Gong, A. Imbault, R. Farnood, *Appl. Catal. B* **2017**, *204*, 296–303.
[41] K. Kamwilaisak, P. C. Wright, *Energy Fuels* **2012**, *26*, 2400–2406.
[42] N. Srisasiwimon, S. Chuangchote, N. Laosiripojana, T. Sagawa, *ACS Sustainable Chem. Eng.* **2018**, *6*, 13968–13976.
[43] L. Tonucci, F. Coccia, M. Bressan, N. D'Alessandro, *Waste Biomass Valorization* **2012**, *3*, 165–174.
[44] V. Nair, P. Dhar, R. Vinu, *RSC Adv.* **2016**, *6*, 18204–18216.
[45] X. Wu, X. Fan, S. Xie, J. Lin, J. Cheng, Q. Zhang, L. Chen, Y. Wang, *Nat. Catal.* **2018**, *1*, 772–780.
[46] Y. Lu, X. Y. Wei, Z. Wen, H. B. Chen, Y. C. Lu, Z. M. Zong, J. P. Cao, S. C. Qi, S. Z. Wang, L. C. Yu, W. Zhao, X. Fan, Y. P. Zhao, *Fuel Process. Technol.* **2014**, *117*, 8–16.
[47] K. Kobayakawa, Y. Sato, S. Nakamura, A. Fujishima, *Bull. Chem. Soc. Jpn.* **1989**, *62*, 3433–3436.
[48] P. Tsapekos, M. Alvarado-Morales, D. Boscaro, M. Mazarji, L. Sartori, I. Angelidaki, *Energy Fuels* **2018**, *32*, 6813–6822.
[49] R. Vinu, G. Madras, *Appl. Catal. A* **2009**, *366*, 130–140.
[50] X. Wu, S. Xie, H. Zhang, Q. Zhang, B. F. Sels, Y. Wang, *Adv. Mater.* **2021**, *33*, 2007129.
[51] S. Liu, N. Zhang, Z. R. Tang, Y. J. Xu, *ACS Appl. Mater. Interfaces* **2012**, *4*, 6378–6385.
[52] M. Ko, L. T. M. Pham, Y. J. Sa, J. Woo, T. V. T. Nguyen, J. H. Kim, D. Oh, P. Sharma, J. Ryu, T. J. Shin, S. H. Joo, Y. H. Kim, J. W. Jang, *Nat. Commun.* **2019**, *10*, 5123.
[53] M. Tian, J. Wen, D. MacDonald, R. M. Asmussen, A. Chen, *Electrochem. Commun.* **2010**, *12*, 527–530.
[54] H. Fuse, H. Nakao, Y. Saga, A. Fukatsu, M. Kondo, S. Masaoka, H. Mitsunuma, M. Kanai, *Chem. Sci.* **2020**, *11*, 12206–12211.

[55] J. D. Nguyen, B. S. Matsuura, C. R. J. Stephenson, *J. Am. Chem. Soc.* **2014**, *136*, 1218–1221.
[56] I. Bosque, G. Magallanes, M. Rigoulet, M. D. Kärkäs, C. R. J. Stephenson, *ACS Cent. Sci.* **2017**, *3*, 621–628.
[57] J. Schwarz, B. König, *Chem. Commun.* **2019**, *55*, 486–488.
[58] M. D. Kärkäs, I. Bosque, B. S. Matsuura, C. R. J. Stephenson, *Org. Lett.* **2016**, *18*, 5166–5169.
[59] Z. Hao, S. Li, J. Sun, S. Li, F. Zhang, *Appl. Catal. B* **2018**, *237*, 366–372.
[60] N. Luo, M. Wang, H. Li, J. Zhang, H. Liu, F. Wang, *ACS Catal.* **2016**, *6*, 7716–7721.
[61] N. Luo, M. Wang, H. Li, J. Zhang, T. Hou, H. Chen, X. Zhang, J. Lu, F. Wang, *ACS Catal.* **2017**, *7*, 4571–4580.
[62] G. Han, T. Yan, W. Zhang, Y. C. Zhang, D. Y. Lee, Z. Cao, Y. Sun, *ACS Catal.* **2019**, *9*, 11341–11349.
[63] M. Wang, J. Lu, J. Ma, Z. Zhang, F. Wang, *Angew. Chem. Int. Ed.* **2015**, *54*, 14061–14065.
[64] T. Hou, N. Luo, H. Li, M. Heggen, J. Lu, Y. Wang, F. Wang, *ACS Catal.* **2017**, *7*, 3850–3859.
[65] H. Liu, H. Li, J. Lu, S. Zeng, M. Wang, N. Luo, S. Xu, F. Wang, *ACS Catal.* **2018**, *8*, 4761–4771.
[66] A. Du, S. Sanvito, Z. Li, D. Wang, Y. Jiao, T. Liao, Q. Sun, Y. H. Ng, Z. Zhu, R. Amal, S. C. Smith, *J. Am. Chem. Soc.* **2012**, *134*, 4393–4397.
[67] S. T. Nguyen, P. R. D. Murray, R. R. Knowles, *ACS Catal.* **2020**, *10*, 800–805.
[68] Y. Wang, J. He, Y. Zhang, *CCS Chem.* **2020**, *2*, 107–117.
[69] H. Liu, H. Li, N. Luo, F. Wang, *ACS Catal.* **2020**, *10*, 632–643.
[70] Y. Wang, Y. Liu, J. He, Y. Zhang, *Sci. Bull.* **2019**, *64*, 1658–1666.
[71] S. Gazi, W. K. Hung Ng, R. Ganguly, A. M. Putra Moeljadi, H. Hirao, H. sen Soo, *Chem. Sci.* **2015**, *6*, 632–643.
[72] S. Li, Z. Hao, K. Wang, M. Tong, Y. Yang, H. Jiang, Y. Xiao, F. Zhang, *Chem. Commun.* **2020**, *56*, 11243–11246.
[73] J. Luo, J. Zhang, *J. Org. Chem.* **2016**, *81*, 9131–9137.
[74] C. Costentin, M. Robert, J. M. Savéant, *Organic Electrochemistry*, Fifth Edition: Revised and Expanded, Taylor & Francis, New York, **2015**, pp. 481–510.
[75] G. Zhang, G. Kim, W. Choi, *Energy Environ. Sci.* **2014**, *7*, 954–966.
[76] T. Werpy, G. Petersen, *Office of Scientific and Technical Information 2004*, U.S. Department of Energy (DOE), Golden, CO, Report DOE/GO-102004-1992, **2004**.
[77] L. Wang, Z. Zhang, L. Zhang, S. Xue, W. O. S. Doherty, I. M. O'Hara, X. Ke, *RSC Adv.* **2015**, *5*, 5242–85247.
[78] J. Zou, G. Zhang, X. Xu, *Appl. Catal. A* **2018**, *563*, 73–79.
[79] H. Hao, L. Zhang, W. Wang, S. Zeng, *ChemSusChem* **2018**, *11*, 2810–2817.
[80] L. Zhang, W. Wang, S. Zeng, Y. Su, H. Hao, *Green Chem.* **2018**, *20*, 3008–3013.
[81] A. Speltini, M. Sturini, D. Dondi, E. Annovazzi, F. Maraschi, V. Caratto, A. Profumo, A. Buttafava, *Photochem. Photobiol. Sci.* **2014**, *13*, 1410–1419.
[82] J. C. Colmenares, A. Magdziarz, A. Bielejewska, *Bioresour. Technol.* **2011**, *102*, 11254–11257.
[83] R. Chong, J. Li, Y. Ma, B. Zhang, H. Han, C. Li, *J. Catal.* **2014**, *314*, 101–108.
[84] G. Iervolino, V. Vaiano, D. Sannino, L. Rizzo, A. Galluzzi, M. Polichetti, G. Pepe, P. Campiglia, *Int. J. Hydrogen Energy* **2018**, *43*, 2184–2196.
[85] M. Bellardita, E. I. García-López, G. Marcì, L. Palmisano, *Int. J. Hydrogen Energy* **2016**, *41*, 1075–1081.
[86] B. Zhou, J. Song, Z. Zhang, Z. Jiang, P. Zhang, B. Han, *Green Chem.* **2017**, *19*, 1075–1081.
[87] H. F. Ye, R. Shi, X. Yang, W. F. Fu, Y. Chen, *Appl. Catal. B* **2018**, *233*, 70–79.
[88] A. Allegri, V. Maslova, M. Blosi, A. L. Costa, S. Ortelli, F. Basile, S. Albonetti, *Molecules* **2020**, *25*, 5225.
[89] A. Khan, M. Goepel, A. Kubas, D. Łomot, W. Lisowski, D. Lisovytskiy, A. Nowicka, J. C. Colmenares, R. Gläser, *ChemSusChem* **2021**, *14*, 1351–1362.
[90] Q. Wu, Y. He, H. Zhang, Z. Feng, Y. Wu, T. Wu, *Mol. Catal.* **2017**, *436*, 1351–1362.
[91] H. Zhang, Q. Wu, C. Guo, Y. Wu, T. Wu, *ACS Sustainable Chem. Eng.* **2017**, *5*, 3517–3523.
[92] M. Zhang, Z. Li, X. Xin, J. Zhang, Y. Feng, H. Lv, *ACS Catal.* **2020**, *10*, 14793–14800.
[93] G. Han, Y. H. Jin, R. A. Burgess, N. E. Dickenson, X. M. Cao, Y. Sun, *J. Am. Chem. Soc.* **2017**, *139*, 15584–15587.
[94] A. Caravaca, W. Jones, C. Hardacre, M. Bowker, *Proc. R. Soc. A* **2016**, 20160054.
[95] L. Wang, Z. Zhang, L. Zhang, S. Xue, W. O. S. Doherty, I. M. O'Hara, X. Ke, *RSC Adv.* **2015**, *5*, 85242–85247.
[96] B. Zhang, J. Li, L. Guo, Z. Chen, C. Li, *Appl. Catal. B* **2018**, *237*, 88149–88153.
[97] K. Tsutsumi, N. Kurata, E. Takata, K. Furuichi, M. Nagano, K. Tabata, *Appl. Catal. B* **2014**, *147*, 1009–1014.
[98] J. C. Colmenares, A. Magdziarz, K. Kurzydlowski, J. Grzonka, O. Chernyayeva, D. Lisovytskiy, *Appl. Catal. B* **2013**, 134–135.
[99] J. C. Colmenares, A. Magdziarz, O. Chernyayeva, D. Lisovytskiy, K. Kurzydłowski, J. Grzonka, *ChemCatChem* **2013**, *5*, 136.
[100] L. da Vià, C. Recchi, E. O. Gonzalez-Yañez, T. E. Davies, J. A. Lopez-Sanchez, *Appl. Catal. B* **2017**, *202*, 281–288.
[101] C. Li, J. Li, L. Qin, P. Yang, D. G. Vlachos, *ACS Catal.* **2021**, *11*, 11336–11359.
[102] L. Cheng, D. Huang, Y. Zhang, Y. Wu, *Appl. Organomet. Chem.* **2021**, *35*, e6404.
[103] A. Lolli, V. Maslova, D. Bonincontro, F. Basile, S. Ortelli, S. Albonetti, *Molecules* **2018**, *23*, 2792.
[104] W. Liang, R. Zhu, X. Li, J. Deng, Y. Fu, *Green Chem.* **2021**, *23*, 6604–6613.
[105] Y. Pellegrin, F. Odobel, *C. R. Chim.* **2017**, *20*, 7581–7593.
[106] L. Zhang, R. Chen, J. Luo, J. Miao, J. Gao, B. Liu, *Nano Res.* **2016**, *9*, 3388–3393.
[107] X. Lu, S. Xie, H. Yang, Y. Tong, H. Ji, *Chem. Soc. Rev.* **2014**, *43*, 7581–7593.
[108] H. Zhao, C. F. Li, L. Y. Liu, B. Palma, Z. Y. Hu, S. Renneckar, S. Larter, Y. Li, M. G. Kibria, J. Hu, B. L. Su, *J. Colloid Interface Sci.* **2021**, *585*, 694–704.
[109] C. Li, H. Wang, S. B. Naghadeh, J. Z. Zhang, P. Fang, *Appl. Catal. B* **2018**, *227*, 229–239.
[110] D. W. Wakerley, M. F. Kuehnel, K. L. Orchard, K. H. Ly, T. E. Rosser, E. Reisner, *Nat. Energy* **2017**, *2*, 17021.
[111] R. Djellabi, R. Giannantonio, E. Falletta, C. L. Bianchi, *Curr. Opin. Chem. Eng.* **2021**, *33*, 100696.
[112] E. Calcio Gaudino, G. Cravotto, M. Manzoli, S. Tabasso, *Chem. Soc. Rev.* **2021**, *50*, 1785–1812.
[113] Reports and Data, "Materials and Chemicals—BTX Market (2016–2027)," can be found under https://www.reportsanddata.com/report-detail/btx-benzene-toluene-and-xylene-market, **2020** (accessed 1 September 2022).
[114] Valuates Reports, "Global Phenol Derivatives Market Insights, Forecast to 2028," can be found under https://reports.valuates.com/market-reports/QYRE-Auto-17Q10320/global-phenol-derivatives, **2022** (accessed 13 October 2022).
[115] Reports and Data, "Market and Chemicals-Adipic acid Market (2018–2028)," can be found under https://www.reportsanddata.com/report-detail/adipic-acid-market, **2018** (accessed 1 September 2022).
[116] Grand View Research, "Sorbitol Market Growth & Trends 2021–2028," can be found under https://www.grandviewre-

search.com/press-release/global-sorbitol-market, **2021** (accessed 1 September 2022).
[117] Reports and Data, "Materials and Chemicals - Glucaric Acid Market (2019–2027)," can be found under https://www.reportsanddata.com/report-detail/glucaric-acid-market, **2020** (accessed 1 September 2022).
[118] Reports and Data, 122. "Gluconic Acid Market" can be found under https://www.reportsanddata.com/report-detail/gluconic-acid-market, **2021** (accessed 1 September 2022).
[119] Credence Research Report, "Fumaric Acid Market (2016–2028)" can be found under https://www.credenceresearch.com/report/fumaric-acid-market, **2022** (accessed 1 September 2022).
[120] J. Wei, Q. Yuan, T. Wang, L. Wang, *Front. Chem. Eng. China* **2010**, *4*, 57–64.
[121] Reports and Data, "Materials and Chemicals—2,5-Furandicarboxylic Acid (FDCA) Market(2020–2028)," can be found under https://www.reportsanddata.com/report-detail/2–5-furandicarboxylic-acid-fdca-market, **2020** (accessed 10 November 2022).
[122] Grand Review Research, "Furfuryl Alcohol Market" can be found under https://www.grandviewresearch.com/industry-analysis/furfuryl-alcohol-market, **2021** (accessed 1 September 2022).
[123] Grand Review Research, "Vanillin Market Size, Share & Trends Analysis Report by End-use" can be found under https://www.grandviewresearch.com/industry-analysis/vanillin-market, **2021** (accessed 10 December 2022).
[124] Research Market., "Global Vanillin Market Report (2020–2027)," can be found under https://www.marketresearch.com/Global-Industry-Analysts-v1039/Vanillin-14407427/, **2021** (accessed 10 December 2022).
[125] Reports and Data, "Materials and Chemicals—Resorcinol Market Reports and Data (2018–2028)," can be found under https://www.reportsanddata.com/report-detail/resorcinol-market, **2018** (accessed 1 September 2022).
[126] Transparency Market Research, "Cresols market size, sales, share and forecasts by 2027," can be found under https://www.transparencymarketresearch.com/cresols-market.html **2020** (accessed 1 September 2022).
[127] The Express Digital Report, "Guaiacol Market Size for the Period 2022–2028" can be found under https://www.digitaljournal.com/pr/guaiacol-market-size-is-expected-to-grow-at-a-cagr-of-1–31-during-assessment-period-2022-2028-114-report-pages, **2022** (accessed 10 December 2022).
[128] Grand Review Research, "Levulinic Acid Market Size, Share & Trends Analysis Report (2015–2020)" can be found under https://www.grandviewresearch.com/industry-analysis/levulinic-acid-market, **2021** (accessed 10 December 2022).
[129] L. A. dos Santos, G. V. das Fraga, D. A. Pontes, L. M. A. Campos, L. A. M. Pontesa, L. S. G. Teixeirad, *Quim. Nova* **2021**, *44*, 1300–1310.
[130] 360 Research Reports, "Global 5-hydroxymethylfurfural Market Research Report", can be found under https://www.360marketupdates.com/global-5-hydroxymethylfurfural-5-hmf-cas-67-47-0-market-17210331, **2022** (accessed 10 December 2022).
[131] Y. Cao, N. Wang, X. He, H. R. Li, L. N. He, *ACS Sustainable Chem. Eng.* **2018**, *6*, 15032–15039.
[132] C. Bie, L. Wang, J. Yu, *Chem* **2022**, *8*, 1567–1574.
[133] M. Yasuda, A. Miura, R. Yuki, Y. Nakamura, T. Shiragami, Y. Ishii, H. Yokoi, *J. Photochem. Photobiol. A* **2011**, *220*, 195–199.
[134] L. Shiamala, K. Alamelu, V. Raja, B. M. Jaffar Ali, *J. Environ. Chem. Eng.* **2018**, *6*, 3306–3321.
[135] K. Wu, M. Cao, Q. Zeng, X. Li, *Green Energy Environ.* **2022**, *7*, 383–405.
[136] G. Chatel, S. Valange, R. Behling, J. C. Colmenares, *ChemCatChem* **2017**, *9*, 2615–2621.
[137] P. Chen, W. Cui, H. Wang, X. Dong, J. Li, Y. Sun, Y. Zhou, Y. Zhang, F. Dong, *Appl. Catal. B* **2020**, *272*, 118977.
[138] D. Aboagye, F. Medina, S. Contreras, *Catal. Today* **2022**, *383*, 225–264.
[139] F. Yang, M. A. Hanna, R. Sun, *Biotechnol. Biofuels* **2012**, *5*, 1–10.
[140] G. Iervolino, I. Zammit, V. Vaiano, L. Rizzo, *Top. Curr. Chem.* **2020**, *378*, 225–264.
[141] L. Wang, Q. Zhang, B. Chen, Y. Bu, Y. Chen, J. Ma, F. L. Rosario-Ortiz, R. Zhu, *Water Res.* **2020**, *174*, 115605.
[142] M. Y. Qi, M. Conte, M. Anpo, Z. R. Tang, Y. J. Xu, *Chem. Rev.* **2021**, *121*, 13051–13085.
[143] A. V. Puga, *Coord. Chem. Rev.* **2016**, *315*, 1–66.
[144] J. Bachér, E. Pohjalainen, E. Yli-Rantala, K. Boonen, D. Nelen, *Environmental Aspects Related to the Use of Critical Raw Materials in Priority Sectors and Value Chains*, **2020**, pp. 18–20.
[145] E. Friehs, Y. AlSalka, R. Jonczyk, A. Lavrentieva, A. Jochums, J. G. Walter, F. Stahl, T. Scheper, D. Bahnemann, *J. Photochem. Photobiol. C* **2016**, *29*, 1409–1420.
[146] N. M. Zaki, N. Tirelli, *Expert Opin. Drug Delivery* **2010**, *7*, 895–913.
[147] B. Yameen, W. Il Choi, C. Vilos, A. Swami, J. Shi, O. C. Farokhzad, *J. Controlled Release* **2014**, *190*, 485–499.
[148] S. Rajendran, R. Raghunathan, I. Hevus, R. Krishnan, A. Ugrinov, M. P. Sibi, D. C. Webster, J. Sivaguru, *Angew. Chem. Int. Ed.* **2015**, *54*, 1159–1163.
[149] X. Wu, J. Li, S. Xie, P. Duan, H. Zhang, J. Feng, Q. Zhang, J. Cheng, Y. Wang, *Chem* **2020**, *6*, 3038–3053.
[150] J. C. Colmenares, R. S. Varma, V. Nair, *Chem. Soc. Rev.* **2017**, *46*, 6675–6686.
[151] J. Yue, *Chem. Eng. Process.* **2022**, *177*, 108986.

Manuscript received: February 7, 2023
Accepted manuscript online: May 10, 2023
Version of record online: May 31, 2023